NASA/CR—2004-213116

Analysis of Fuel Vaporization, Fuel-Air Mixing, and Combustion in Integrated Mixer-Flame Holders

J.M. Deur
NYMA, Inc., Brook Park, Ohio

M.C. Cline
Los Alamos National Laboratory, Los Alamos, New Mexico

July 2004

The NASA STI Program Office . . . in Profile

Since its founding, NASA has been dedicated to the advancement of aeronautics and space science. The NASA Scientific and Technical Information (STI) Program Office plays a key part in helping NASA maintain this important role.

The NASA STI Program Office is operated by Langley Research Center, the Lead Center for NASA's scientific and technical information. The NASA STI Program Office provides access to the NASA STI Database, the largest collection of aeronautical and space science STI in the world. The Program Office is also NASA's institutional mechanism for disseminating the results of its research and development activities. These results are published by NASA in the NASA STI Report Series, which includes the following report types:

- TECHNICAL PUBLICATION. Reports of completed research or a major significant phase of research that present the results of NASA programs and include extensive data or theoretical analysis. Includes compilations of significant scientific and technical data and information deemed to be of continuing reference value. NASA's counterpart of peer-reviewed formal professional papers but has less stringent limitations on manuscript length and extent of graphic presentations.

- TECHNICAL MEMORANDUM. Scientific and technical findings that are preliminary or of specialized interest, e.g., quick release reports, working papers, and bibliographies that contain minimal annotation. Does not contain extensive analysis.

- CONTRACTOR REPORT. Scientific and technical findings by NASA-sponsored contractors and grantees.

- CONFERENCE PUBLICATION. Collected papers from scientific and technical conferences, symposia, seminars, or other meetings sponsored or cosponsored by NASA.

- SPECIAL PUBLICATION. Scientific, technical, or historical information from NASA programs, projects, and missions, often concerned with subjects having substantial public interest.

- TECHNICAL TRANSLATION. English-language translations of foreign scientific and technical material pertinent to NASA's mission.

Specialized services that complement the STI Program Office's diverse offerings include creating custom thesauri, building customized databases, organizing and publishing research results . . . even providing videos.

For more information about the NASA STI Program Office, see the following:

- Access the NASA STI Program Home Page at ***http://www.sti.nasa.gov***

- E-mail your question via the Internet to help@sti.nasa.gov

- Fax your question to the NASA Access Help Desk at 301–621–0134

- Telephone the NASA Access Help Desk at 301–621–0390

- Write to:
  NASA Access Help Desk
  NASA Center for AeroSpace Information
  7121 Standard Drive
  Hanover, MD 21076

NASA/CR—2004-213116

Analysis of Fuel Vaporization, Fuel-Air Mixing, and Combustion in Integrated Mixer-Flame Holders

J.M. Deur
NYMA, Inc., Brook Park, Ohio

M.C. Cline
Los Alamos National Laboratory, Los Alamos, New Mexico

Prepared under Contract NAS3–27235

National Aeronautics and
Space Administration

Glenn Research Center

July 2004

Document History

This research was originally published internally as HSR031 in April 1996.

Note that at the time of research, the NASA Lewis Research Center
was undergoing a name change to the
NASA John H. Glenn Research Center at Lewis Field.
Both names may appear in this report.

Available from

NASA Center for Aerospace Information
7121 Standard Drive
Hanover, MD 21076

National Technical Information Service
5285 Port Royal Road
Springfield, VA 22100

Available electronically at http://gltrs.grc.nasa.gov

Analysis of Fuel Vaporization, Fuel-Air Mixing, and Combustion in Integrated Mixer-Flame Holders

J.M. Deur
NYMA, Inc.
Brook Park, Ohio 44142

M.C. Cline
Los Alamos National Laboratory
Los Alamos, New Mexico

Abstract

Requirements to limit pollutant emissions from the gas turbine engines for the future High-Speed Civil Transport (HSCT) have led to consideration of various low-emission combustor concepts. One such concept is the Integrated Mixer-Flame Holder (IMFH). This report describes a series of IMFH analyses performed with KIVA-II, a multi-dimensional CFD code for problems involving sprays, turbulence, and combustion. To meet the needs of this study, KIVA-II's boundary condition and chemistry treatments are modified. The study itself examines the relationships between fuel vaporization, fuel-air mixing, and combustion. Parameters being considered include: mixer tube diameter, mixer tube length, mixer tube geometry (converging-diverging versus straight walls), air inlet velocity, air inlet swirl angle, secondary air injection (dilution holes), fuel injection velocity, fuel injection angle, number of fuel injection ports, fuel spray cone angle, and fuel droplet size. Cases are run with and without combustion to examine the variations in fuel-air mixing and potential for flashback due to the above parameters. The degree of fuel-air mixing is judged by comparing average, minimum, and maximum fuel/air ratios at the exit of the mixer tube, while flame stability is monitored by following the location of the flame front as the solution progresses from ignition to steady state. Results indicate that fuel-air mixing can be enhanced by a variety of means, the best being a combination of air inlet swirl and a converging-diverging mixer tube geometry. With the IMFH configuration utilized in the present study, flashback becomes more common as the mixer tube diameter is increased and is instigated by disturbances associated with the dilution hole flow.

Background

Nitrogen oxides (NO_x) are serious contributors to air pollution, and considerable engineering effort is being expended to reduce their emission from the gas turbine combustors of the future HSCT. Lean combustion concepts are one means of achieving low emissions, as NO_x formation is reduced substantially at low equivalence ratios. Lean premixed-prevaporized (LPP) systems (Fig. 1A) separate the fuel vaporization and fuel-air mixing processes from the final combustion process. This eliminates non-uniformities in the fuel-air mixture, which eliminates hot spots where high levels of NO_x are formed. Unfortunately, lean combustion devices have some drawbacks, particularly with regards to flame stability.[1]

The IMFH is one means of incorporating the LPP concept into a gas turbine engine combustor. However, several IMFH fuel-air mixing and flame stability issues are yet to be fully resolved, making detailed analysis of IMFH configurations a high priority.[2]

The present series of calculations examines the role of IMFH geometry and various inflow parameters on fuel-air mixture uniformity and flame stability. These analyses start with the cylindrical configuration consisting of a straight tube with a "hypodermic needle" fuel injector adopted for the LPP sector rig (Fig. 1B).[3] To reduce computational costs, only a single IMFH tube is considered. The downstream area change for the dump region of this single tube is calculated by dividing the dump area shared by all of the IMFH tubes in the sector rig by the number of tubes.

Numerical Method

The calculations are performed with KIVA-II, a CFD program developed originally to study the in-cylinder combustion dynamics of internal combustion engines.[4] However, because the code can treat problems combining sprays, turbulence, and combustion, it can be employed in the analysis of gas turbine combustors as well.[5,6]

KIVA-II describes fuel sprays with a stochastic

model applied to discrete computational particles representing collections of droplets with identical physical properties (size, temperature, velocity, etc.). These particles interact with the surrounding fluid, exchanging mass, momentum, and energy as the droplets travel downstream and evaporate. The spray model also incorporates sub-models for droplet collisions, turbulent dispersion, and aerodynamic breakup. In practice, the collision and breakup sub-models are often too efficient, rapidly skewing droplet distributions to the smaller sizes in an unrealistic fashion. As a result, these two models are not used here.

To characterize turbulence within the flowfield, KIVA-II employs a standard k-ε model with wall functions.

KIVA-II can accept an arbitrary reaction set and incorporates a quasi-equilibrium option to split fast and slow reactions between equilibrium and finite-rate kinetics, respectively. However, as originally released, KIVA-II is limited to laminar kinetics. For this study, the mixing-controlled combustion model of Magnussen and Hjertager is added to portray the combustion-turbulence interaction.[7] This model is used in conjunction with the simplified reaction scheme developed by Ying and Nguyen to describe propane combustion.[8] Thus, while the fuel (Jet-A) has the physical properties (vapor pressure, latent heat, etc.) of Jet-A when it is in the liquid state, it is treated as propane once vaporized.

Owing to its origins, KIVA-II's ability to treat some of the geometries to be examined in this study is also limited. To rectify this, the program's boundary condition treatment is revised to allow incorporation of dilution jets, non-vertical walls, and inflow-outflow boundary planes with mixtures of open and closed grid cells.

Grids and Boundary Conditions

A variety of grids are used in this study, almost all generated with KIVA-II's internal grid generation routines. The grid for the baseline case (Figs. 2A and 2B) is a uniform cylindrical mesh. Due to symmetry about the plane passing through the fuel injection tube, only a 180° half-cylinder is needed, leading to a 27x19x205 mesh in cases when the dump section is included and a 11x19x151 mesh when only the mixer tube is analyzed. Cell spacing is chosen, in part, such that the dilution holes near the mixer tube exit can be approximated by 2x2 clusters of cells. The rectangle formed by these cells has 93% of the area and 93% of the width of the original circular dilution hole.

To test some geometry variables and inlet conditions, the baseline grid has to be modified. For cases involving converging-diverging mixer tubes, radial cell spacing in successive K-planes (I, J, and K grid indices correspond to r, θ, and z directions in cylindrical coordinates) is linearly varied to produce the desired venturi geometry. Cases involving inlet air swirl require full 360° grids, since the symmetry plane is lost.

To study the flow blockage associated with the fuel injection tube, an externally generated grid is employed that explicitly includes the tube (Fig. 2C). To reduce grid effects and return to the cell spacing needed to represent the downstream dilution holes, the grid is slowly returned to the original baseline configuration over several K-planes downstream of the injection tube.

For all cases examined, the air inlet temperature and pressure are 1100° F and 11.5 atm, respectively. For the baseline case, the total air mass flow rate is 0.161 lbm/sec, with 88.5% of the flow entering through the base of the mixer tube and the remainder split equally amongst the dilution holes ringing the tube near its downstream exit. The overall fuel/air ratio is 0.033. The fuel is injected at a velocity of 52.7 fps, with a droplet SMD of 20 μm and a spray cone angle of 20°.[9]

Analysis

To quantify the degree of mixing, three exit plane fuel/air ratios are calculated: minimum, maximum, and average. The first two are simply the minimum and maximum values found amongst the grid cells located at the exit plane of the mixer tube, while the average value is a spatial or cell average across the exit plane. The spatial average is more revealing than the mass average, since the latter just equals the overall fuel/air ratio, a constant in these calculations. On the other hand, the spatial average varies with the distribution of fuel vapor across the exit plane owing to the variation in cell density. If the fuel is concentrated near the center of the tube (Region A in Fig. 2D), the average is relatively high, since there is a greater cell density near the tube's center. However, if there is more fuel near the wall (Region B), the average is relatively low, due to the lower cell density near the wall.

In all cases, the three reported fuel/air ratios are averages over a number of cycles, typically 1,000, to account for the random changes in the fuel/air ratio at the exit plane due to the stochastic spray model. Since the distribution of droplets intro-

duced by the spray model changes as a random variable, the fuel-air distribution also changes over time. This can be seen in the time histories of the average and maximum exit plane fuel/air ratios (Fig. 3) and fuel droplet distributions at various time points (Figs. 4, 5, and 6) for the baseline case.

Results

To date, 50 IMFH analyses have been completed (Table 1), examining the effects of a variety of parameters on fuel-air mixing and combustion.

Modeling Considerations

Numerical Effects

As noted above, KIVA-II simulates spray droplets as collections of computational particles. The accuracy of this depiction increases as more particles are used. However, more particles require more memory and more computations, so a balance has to be struck between accuracy and cost. As comparisons between baseline cases run with injection rates of computational particles of 10^6 and 10^7 particles per second (pps) show only minor differences in results (Fig. 7), the 10^6 pps rate is used throughout this series of analyses.

Numerical accuracy is also strongly dependent on grid resolution. Comparison of results obtained with the previously described 11x19x151 grid and a finer 17x19x151 grid with logarithmic cell spacing near the tube wall show only minor differences for the baseline case (Fig. 8). The variation in the average exit plane fuel/air ratio is a result of the redistribution of cells due to the logarithmic spacing in the fine grid.

Fuel Injection Tube

In most of the calculations presented here, the flow blockage due to the fuel injection tube is not represented. To examine what effect this blockage has on fuel-air mixing, an analysis of the baseline configuration with the fuel injection tube included is performed to allow a side-by-side comparison to be made (Fig. 9). While the axial velocity field immediately behind the injection tube is significantly disturbed, there is little effect on the fuel spray pattern and, consequently, relatively little effect on the fuel-air distribution. While there is some enhanced mixing on that side of the mixer tube downstream of the injection tube, there is insufficient fuel there to strongly effect the overall fuel-air distribution.

Fuel-Air Mixing

Fuel Droplets and Sprays

In the next series of analyses, the fuel injection angle is varied from the baseline's 15° to 90°, i.e., from roughly perpendicular to the inlet air flow to parallel to that flow (Fig. 10). Initially, there is relatively little change, until the angle increases to where the spray impingement on the mixer tube wall is eliminated. As the angle increases from that point, there is substantial improvement in overall mixture uniformity. The star-shaped pattern in the exit plane fuel/air ratio at 90° (Fig. 10B) results from the dilution hole inflow.

A similar improvement in uniformity is obtained by reducing the fuel injection velocity (Fig.11). Curiously, increasing the injection velocity also reduces the maximum exit plane fuel/air ratio. However, the minimum fuel/air ratio in this case is reduced far more, indicating that overall non-uniformity at the higher injection velocity is still increased. The decrease in the maximum fuel/air ratio may be a result of the higher velocity displacing the spray cone outward such that the mixer tube wall cuts across a broader section of the cone, thus spreading the fuel across a wider arc along the tube wall.

Perhaps surprisingly, droplet size has little effect on mixing, at least over the range of sizes considered here (Fig. 12). However, the fuel droplet population results suggest that uniformity will increase with even smaller droplets, since it appears that vaporization becomes so fast that wall impingement will be avoided altogether. Of course, such small sizes may not be physically realizable.

These last two series of calculations point to an unexpected advantage of numerical analysis. Given the structure of KIVA-II, it is possible to vary independently parameters that, in reality, are closely coupled, e.g., fuel injection velocity and fuel droplet SMD. This permits separate evaluations of these parameters to be made that may be difficult to perform experimentally.

The final spray parameter to be considered is the spray cone angle (Fig. 13). As might be expected, increasing the cone angle improves the degree of fuel-air mixing.

Air Inflow

Turning to modifications of the air inflow, the first set of analyses examines the addition of a venturi effect (Fig. 14). In this series, the throat of the venturi is at the same axial station as the fuel

injection. The level of constriction is described by the ratio of the minimum to maximum tube radii. Three ratios, from 0.5 to 0.75, are considered here. As anticipated, increasing the throat constriction significantly increases the fuel-air mixture uniformity at the exit plane of the mixer tube. However, aerodynamic choking at the throat limits the degree of constriction permissible. In this investigation, the flow chokes in the 0.5 radius ratio tube.

Inlet air swirl is another means of improving fuel-air mixing. Swirl angles from 30° to 60° are considered in this study (Fig. 15), with the best mixing found at the highest angle.

In practice, swirl and venturi effects are often combined. Unfortunately, the baseline conditions in the present study make contemplating this combination difficult, since even modest amounts of swirl combined with the flow acceleration due to the venturi's flow constriction lead to choked flow under the baseline inflow conditions. In fact, only one combination of the parameter values previously considered separately in this study avoids choking (Fig.16). However, this case does demonstrate that the combination of swirl with the venturi flow constriction can improve mixing over either alone.

Dilution Holes

Calculations show that relocating the dilution holes from near the mixer tube exit to the axial station where the fuel injection occurs has almost the same effect as an equivalent venturi tube configuration (Fig. 17). By examining the disturbance to the mean flow created by the dilution holes, it is found that they create a 20% reduction in flow area or the equivalent of a 0.9 radius ratio venturi tube.

Removing the dilution holes altogether also affects the degree of mixture uniformity (Fig. 18). First, to maintain the overall fuel/air ratio, the inflow velocity at the base of the mixer tube must be increased, leading to a slight reduction in the degree of penetration of the fuel spray and a small increase in the downstream distance through which the fuel droplets are convected before vaporizing. These same effects result if the fuel injection velocity is reduced. Based on the effect that reducing fuel injection velocity has on mixing (Fig. 11), this increase in the air velocity can be expected to improve the fuel-air distribution at the mixer tube exit, but the exit plane values show that mixing is actually slightly poorer without the dilution holes. Thus, the direct mixing effect that the dilution holes provide outweighs the slight losses due to the lower air inlet velocity at the mixer tube entrance.

Multiple Fuel Nozzles

Increasing the number of fuel injection nozzles substantially improves the fuel-air distribution at the exit of the mixer tube (Fig. 19). An additional case shows that staggering the nozzles, in this instance by an inch, does not appreciably affect the degree of uniformity at the exit plane. The slight increase in non-uniformity is likely due to the downstream displacement of the second nozzle.

Mixer Tube Length

Reducing the mixer tube length moves the fuel injection point closer to the tube exit, consequently leaving less distance for fuel-air mixing to be performed. Calculations in this series show the decreasing uniformity as the mixer tube is shortened (Fig. 20). The results for the 50% baseline case are even poorer than the exit plane plot indicates, since a small number of droplets are leaving the tube without vaporizing. Thus, there is a small amount of fuel unaccounted for in the fuel/air ratios, since their calculation only considers vaporized fuel.

Mixer Tube Diameter

In considering changes in mixer tube diameter, the effect on the mass flow rate of air entering the tube has to be taken into account. Three approaches are considered here:

In the first (Fig. 21), the flow rate is held constant by reducing in the velocity of the air entering the tube.

In the second (Fig. 22), the inlet velocity of the flow entering at the base of the mixer tube is held constant, leading to an increase in the mass flow. To maintain the same flow splits between this inflow and that through the downstream dilution holes, the dilution hole flow is increased proportionately. Likewise, to maintain the same overall fuel/air ratio, the fuel flow rate is also increased.

In the third (Fig. 23), the inlet velocity of the flow entering at the base of the tube is again held constant, but the dilution hole flow is maintained at the baseline flow rate. The fuel flow rate is again adjusted to match the baseline fuel/air ratio.

In all three cases, the degree of non-uniformity increases as the diameter is increased, yet the uniformity differences among the three cases are relatively minor. However, the corresponding pressure drops within the IMFH tubes (Fig. 24) do vary significantly. This is due to a combination of the variations among the mass flow rates and the relative

strengths of the dilution flows.

Similar effects are seen when the pressure drop at the mixer tube exit is added to that within the tube itself (Fig. 25). With the dump included, these calculated pressure drops can be compared to experimental measurements using the following empirical expression:

$$\dot{m} = AC_d\sqrt{2\rho\Delta p}$$

where AC_d for the baseline IMFH tube geometry is approximately 0.16 in^2.[10] For the baseline inflow conditions, the pressure drop based on this equation is 4.61%, which compares favorably to the 4.30% pressure drop found numerically. For the 150% baseline diameter case with the baseline mass flow rates, the pressure drop found with the above expression is 0.911%, which compares with 1.00% found numerically. Comparisons to the remaining cases shown in Fig. 25 are not possible as their altered dilution flows change their AC_d values.

Flashback Results

As decreasing flow velocities and smaller pressure drops promote flashback, the calculations involving mixer tubes of increasing diameter have been extended to include combustion. Excepting the baseline case, all show some evidence of flashback (Table II and Fig. 26), but the flashback is limited to a small region in the vicinity of the dilution holes on either side of the fuel injection plane. The poor fuel-air distribution within the tube probably explains why no flashback is observed around the other dilution holes; there is insufficient fuel to support combustion around them.

Although the exact mechanism for propagating flashback into the mixer tube is not yet clear, a potential explanation can be proposed: It appears that the adverse pressure gradient immediately downstream of the dilution holes leads to a reverse flow region that draws the flame front back into the mixer tube. When the flame enters the tube, it heats a pocket of gas within, causing the flow to accelerate. The faster flow then drives the flame back out of the tube. The flow within the tube then decelerates to the point where the flame can re-enter, beginning the cycle again.

150% Baseline Diameter Mixer Tube

The importance of the dilution holes in establishing flashback within the mixer tube can be seen by examining the combustion behavior in a series of calculations involving the 150% baseline diameter mixer tube (Fig. 27). As might be expected, the case with the baseline mass flow rate and, hence, the lowest flow speed exhibits the strongest flashback. Maintaining the baseline inflow velocity and dilution flow splits leads to a marginal degree of flashback. Reducing the flow blockage due to the dilution holes even more by keeping the baseline inflow velocity and baseline dilution flow rate lessens the extent of flashback even further. Flashback is completely eliminated by deleting the dilution flow altogether.

There is also a periodic behavior exhibited by the observed flashback phenomenon. For the 150% baseline diameter analyses, this is most obvious in the baseline mass flow case (Fig. 28).

If the mixer tube is assumed to be an ideal closed-open cylinder filled with a uniform fuel-air mixture, the longitudinal mode frequencies are:

$$f = \frac{(2n+1)a}{4L},\ n = 0,1,2,...$$

where the tube length (L) is found in Fig. 1 to be 5.5 inches and the acoustic velocity (a) is estimated by thermochemistry calculations to be 1815.6 fps.[11] The fundamental longitudinal mode frequency is approximately 990 Hz. The 2880 Hz frequency seen in the numerical calculations most closely matches the second longitudinal mode which has a frequency of 2971 Hz.

The discrepancy between these frequencies may result, in part, from the non-uniformity of the fuel-air mixture that is ignored in the calculation using the above formula. A more likely cause, however, is the failure in the assumption that the downstream boundary is truly open, i.e., that the acoustic pressure vanishes. (Of course, the assumption that the upstream end approximates a closed boundary, i.e., vanishing acoustic velocity, is perhaps as suspect.) An empirical correction for real closed-open tubes estimates the effective tube length for use in the above frequency formula to be 5.65 inches.[12] This reduces the fundamental frequency to 965 Hz and the second mode frequency to 2895 Hz.

Before leaving this case, it is interesting to note that the details of the combustion process in the dump region appear to have little effect on flashback behavior within the mixer tube. In the present calculation, the ignition source is terminated at ap-

proximately 9 msec (after time points A and B in Fig. 28, but before time points C and D). The ignition source consists of a group of cells located approximately halfway between the mixer tube exit and the exit of the dump region. While the source's effect on the combustion process in the dump region can be seen clearly by comparing the axial velocity, fuel/air ratio, and temperature plots before and after termination, there is little effect on the oscillation frequency, amplitude, or other characteristics of the flashback.

Although the oscillations in the baseline velocity cases are less organized (Fig. 29), they have approximately the same 2880 Hz frequency seen in the baseline mass flow case.

200% Baseline Diameter Mixer Tube

The amplitude of the flashback oscillations increases as the mixer tube diameter is increased to 200% of the baseline, although there remains no coherent growth or decay trend in the amplitude over time (Fig. 30). The frequency of oscillation in the exit plane average temperature drops to approximately 900 Hz, which is slightly lower than that of the corrected first longitudinal mode.

250% Baseline Diameter Mixer Tube

Only when the mixer tube diameter is increased to 250% of the baseline are coherent oscillations in the flashback behavior observed (Fig. 31). Here, a limit cycle is reached following a period of monotonic growth in amplitude over successive periods. The frequency of oscillation obtained from the numerical results is 940 Hz, which is close to the corrected first mode value of 965 Hz noted previously.

As the limit amplitude is approached, the point of maximum penetration of the flame front inside the mixer tube moves farther upstream and eventually beyond the dilution holes (Fig. 31E). However, as with the 150% baseline case, flashback is eliminated when the dilution flow is removed (Fig. 31A).

Summary

The impact of various parameters on the degree of fuel-air mixture uniformity in IMFH mixer tubes is quantified through a series of numerical calculations. The biggest gains in uniformity are achieved through a combination of air inlet swirl and venturi tube geometry. Multiple fuel injection points also promote good mixing. Additional analyses examining flashback in mixer tubes with various diameters and dilution arrangements show that flashback is strongly affected by the presence of the dilution holes near the tube exit.

References

[1]Deur, J. M., Kundu, K. P., Darling, D. D., Cline, M. C., Micklow, G. J., Harper, M. R., and Simons, T. A., "Analysis of Lean Premixed/Prevaporized Combustion with KIVA-II," AIAA Paper 94-3895, August 1994.

[2]Heberling, P., private communications with R. R. Tacina (NASA Lewis Research Center), General Electric Aircraft Engines (GEAE), Cincinatti, Ohio, April 1995.

[3]Deur, J. M., Ed., *HSR Analytical Combustion Research Workshop Proceedings*, NASA Report CP-10095, NASA Lewis Research Center, Cleveland, Ohio, 1991.

[4]Amsden, A. A., O'Rourke, P. J., Butler, T. D., "KIVA-II: A Computer Program for Chemically Reacting Flows with Sprays," LANL Report LA-11560-MS, Los Alamos National Laboratory, Los Alamos, New Mexico, May 1989.

[5]Deur, J. M., Kundu, K. P., Nguyen, H. L., "Applied Analytical Combustion/Emissions Research at the NASA Lewis Research Center: A Progress Report," AIAA Paper 92-3338, July 1992.

[6]Cline, M. C., Deur, J. M., Micklow, G. J., Harper, M. R., and Kundu, K. P., "Computation of the Flowfield in an Annular Gas Turbine Combustor," AIAA Paper 93-2074, June 1993.

[7]Magnussen, B. F., and Hjertager, B. H., "On Mathematical Modeling of Turbulent Combustion with Special Emphasis on Soot Formation and Combustion," *Proceedings of the 16th Symposium on Combustion*, The Combustion Institute, Pittsburgh, Pennsylvania, 1977, pp. 719-729.

[8]Ying, S. L., and Nguyen, H. L., "Numerical Simulation of Jet-A Combustion Approximated by Improved Propane Chemical Kinetics," AIAA Paper 91-1859, June 1991.

[9]Kastl, J., private communications with J. M. Deur, GEAE, Cincinnati, Ohio, April 1994.

[10]Matulaitis, J., private communications with J. M. Deur, GEAE, Cincinnati, Ohio, June 1995.

[11]Gordon, S., and McBride, B. J., *CET93 and CETPC: An Interim Updated Version of the NASA Lewis Computer Program for Calculating Complex Chemical Equilibria with Applications*, NASA Report TM-4557, NASA Lewis Research Center, Cleveland, Ohio, 1994.

[12]Rayleigh, J. W. S., *The Theory of Sound (Vol. 2)*, 2nd Ed., The Macmillan Co., London, 1896.

Table I. Summary of Integrated Mixer-Flame Holder Analyses.

Case	Description	f/a_{min}	$f/a_{avg} \times 10^{-2}$	$f/a_{max} \times 10^{-1}$	Remarks
	Cases without Dump Section				
1	Baseline	2.1597×10^{-8}	2.6903	2.7039	$\Delta p = 2.98\%$
2	Baseline with High Computational Droplet Parcel Injection Rate (10^7 pps vs. 10^6 pps)	3.7550×10^{-8}	2.7105	2.6670	
3	Baseline with Fine Grid (17x19x151 vs. 11x19x151)	5.8447×10^{-8}	2.8918	2.7209	$\Delta p = 2.92\%$
4	Baseline with Injection Tube	3.7385×10^{-5}	2.9617	2.4949	
5	Fuel Injection Angle = 45°	2.6170×10^{-8}	2.7389	2.6609	
6	Fuel Injection Angle = 75°	2.6637×10^{-7}	4.4655	2.1535	
7	Fuel Injection Angle = 90°	2.9765×10^{-4}	5.2166	1.2620	
8	Fuel Injection Velocity = 13.2 fps (25% Baseline)	2.1957×10^{-7}	4.2111	1.8509	
9	Fuel Injection Velocity = 26.4 fps (50% Baseline)	6.7068×10^{-8}	3.3612	2.0005	
10	Fuel Injection Velocity = 79.1 fps (150% Baseline)	4.8816×10^{-9}	2.4879	2.4279	
11	Fuel Droplet SMD = 10 μm (50% Baseline)	2.6918×10^{-8}	2.7739	2.3131	
12	Fuel Droplet SMD = 30 μm (150% Baseline)	6.6309×10^{-9}	2.6183	2.7366	
13	Fuel Droplet SMD = 40 μm (200% Baseline)	6.4358×10^{-9}	2.3593	2.4803	
14	Fuel Spray Cone Angle = 40° (200% Baseline)	2.0279×10^{-8}	2.7085	2.3576	
15	Fuel Spray Cone Angle = 60° (300% Baseline)	2.7403×10^{-8}	2.9173	2.0339	
16	Venturi with $r_{min}/r_{max} = 0.50$	—	—	—	Choked Flow
17	Venturi with $r_{min}/r_{max} = 0.67$	2.0949×10^{-4}	3.2765	1.4479	
18	Venturi with $r_{min}/r_{max} = 0.75$	1.9695×10^{-6}	2.7397	1.7951	
19	Inlet Air Swirl Angle = 30°	1.2793×10^{-5}	3.2689	1.2340	
20	Inlet Air Swirl Angle = 45°	1.9663×10^{-4}	3.5690	0.9629	
21	Inlet Air Swirl Angle = 60°	2.4735×10^{-3}	3.6908	0.7594	

Table I. Summary of Integrated Mixer-Flame Holder Analyses (Continued).

Case	Description	f/a_{min}	$f/a_{avg} \times 10^{-2}$	$f/a_{max} \times 10^{-1}$	Remarks
22	Venturi with r_{min}/r_{max} = 0.67 and Inlet Air Swirl Angle = 30°	—	—	—	Choked Flow
23	Venturi with r_{min}/r_{max} = 0.67 and Inlet Air Swirl Angle = 45°	—	—	—	Choked Flow
24	Venturi with r_{min}/r_{max} = 0.67 and Inlet Air Swirl Angle = 60°	—	—	—	Choked Flow
25	Venturi with r_{min}/r_{max} = 0.75 and Inlet Air Swirl Angle = 30°	2.1444×10^{-4}	3.2323	0.8606	
26	Venturi with r_{min}/r_{max} = 0.75 and Inlet Air Swirl Angle = 45°	—	—	—	Choked Flow
27	Venturi with r_{min}/r_{max} = 0.75 and Inlet Air Swirl Angle = 60°	—	—	—	Choked Flow
28	Coplanar Fuel Injection Nozzle and Dilution Holes	1.4749×10^{-5}	2.9546	2.1826	
29	No Dilution Holes	6.5459×10^{-9}	2.5602	2.8792	
30	2 Fuel Injection Nozzles (with 1 Inch Axial Stagger)	1.6801×10^{-5}	3.1653	1.1776	
31	2 Fuel Injection Nozzles (Coplanar)	4.1168×10^{-5}	3.2658	1.0297	
32	4 Fuel Injection Nozzles (Coplanar)	1.9022×10^{-3}	4.3945	0.8327	
33	Mixer Tube Length = 2.75 in (50% Baseline)	6.3107×10^{-11}	2.5576	4.3819	
34	Mixer Tube Length = 4.14 in (75% Baseline)	2.0103×10^{-9}	2.5349	3.3000	
35	Mixer Tube Diameter = 0.75 in with m_{air} = c (150% Baseline)	3.6792×10^{-8}	2.5327	3.6781	Δp = 0.57%
36	Mixer Tube Diameter = 1.00 in with m_{air} = c (200% Baseline)	1.4869×10^{-9}	2.4971	4.0303	Δp = 0.23%
37	Mixer Tube Diameter = 1.25 in with m_{air} = c (250% Baseline)	2.2122×10^{-9}	2.3595	3.7886	
38	Mixer Tube Diameter = 0.75 in with v_{air} = c and Baseline Air Flow Splits (150% Baseline)	6.6383×10^{-12}	2.6131	3.7119	Δp = 2.99%
39	Mixer Tube Diameter = 1.00 in with v_{air} = c and Baseline Air Flow Splits (200% Baseline)	9.4127×10^{-15}	2.5139	4.5456	Δp = 3.03%
40	Mixer Tube Diameter = 0.75 in with v_{air} = c and Baseline Dilution Flow (150% Baseline)	1.4995×10^{-12}	2.5824	3.8694	Δp = 1.55%
41	Mixer Tube Diameter = 1.00 in with v_{air} = c and Baseline Dilution Flow (200% Baseline)	1.5148×10^{-16}	2.4825	4.6879	Δp = 0.95%
Cases with Dump Section					
42	Baseline (without Combustion)	2.5784×10^{-8}	2.7275	2.8820	Δp = 4.30%

Table I. Summary of Integrated Mixer-Flame Holder Analyses (Continued).

Case	Description	f/a_{min}	$f/a_{avg} \times 10^{-2}$	$f/a_{max} \times 10^{-1}$	Remarks
43	Baseline (with Combustion)	1.6875×10^{-8}	2.7103	3.0010	No Flashback
44	Mixer Tube Diameter = 0.75 in with m_{air} = c (150% Baseline)	—	—	—	Flashback, Δp = 1.00%
45	Mixer Tube Diameter = 0.75 in with m_{air} = c and No Dilution Holes (150% Baseline)	—	—	—	Flashback Eliminated
46	Mixer Tube Diameter = 1.00 in with m_{air} = c (200% Baseline)	—	—	—	Flashback
47	Mixer Tube Diameter = 1.25 in with m_{air} = c (250% Baseline)	—	—	—	Flashback
48	Mixer Tube Diameter = 1.25 in with m_{air} = c and No Dilution Holes (250% Baseline)	—	—	—	Flashback Eliminated
49	Mixer Tube Diameter = 0.75 in with v_{air} = c and Baseline Air Flow Splits (150% Baseline)	—	—	—	Flashback, Δp = 3.30%
50	Mixer Tube Diameter = 0.75 in with v_{air} = c and Baseline Dilution Flow (150% Baseline)	—	—	—	Flashback, Δp = 2.25%

Table II. Summary of Integrated Mixer-Flame Holder Combustion Analyses.

Case	Description	Exit Plane Temperature Oscillations		Remarks
		Amplitude	Frequency	
43	Baseline	—	—	No Flashback
44	Mixer Tube Diameter = 0.75 in with m_{air} = c (150% Baseline)	Random	2880 Hz	Flashback
45	Mixer Tube Diameter = 0.75 in with m_{air} = c and No Dilution Holes (150% Baseline)	—	—	Flashback Eliminated
46	Mixer Tube Diameter = 1.00 in with m_{air} = c (200% Baseline)	Random	900 Hz	Flashback
47	Mixer Tube Diameter = 1.25 in with m_{air} = c (250% Baseline)	Limit Cycle	940 Hz	Flashback
48	Mixer Tube Diameter = 1.25 in with m_{air} = c and No Dilution Holes (250% Baseline)	—	—	Flashback Eliminated
49	Mixer Tube Diameter = 0.75 in with v_{air} = c and Baseline Air Flow Splits (150% Baseline)	Random	~2880 Hz	Limited Flashback
50	Mixer Tube Diameter = 0.75 in with v_{air} = c and Baseline Dilution Flow (150% Baseline)	Random	~2880 Hz	Limited Flashback

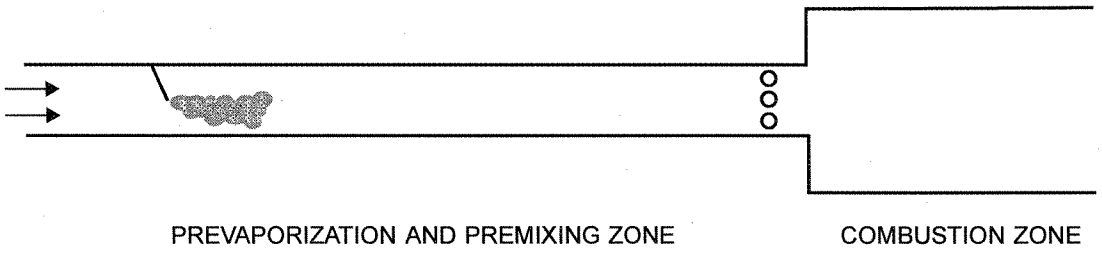

A. Schematic Diagram.

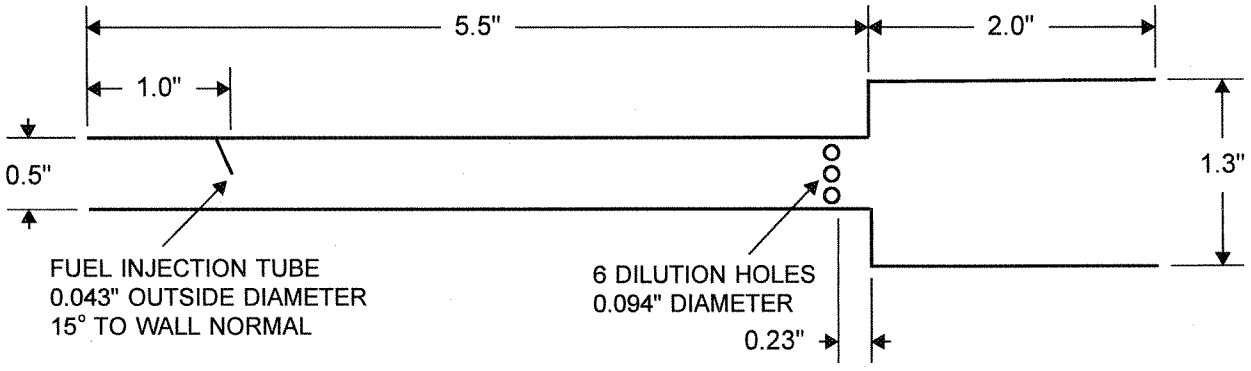

B. Dimensions for Baseline Case.

Figure 1. Integrated Mixer-Flame Holder.

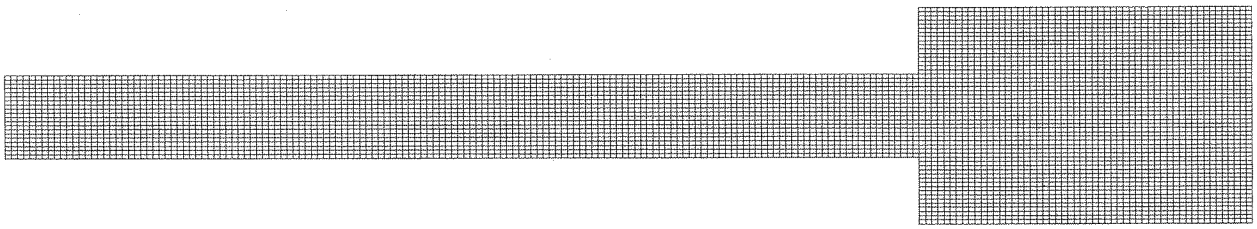

A. J-Plane.

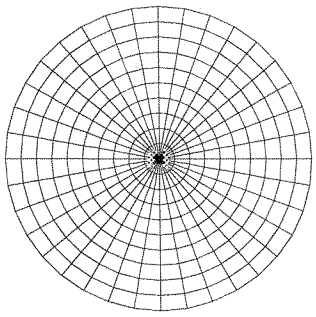

B. K-Plane without Fuel Tube.

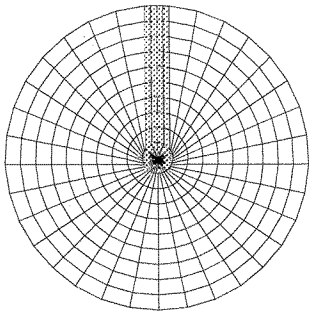

C. K-Plane with Fuel Tube.

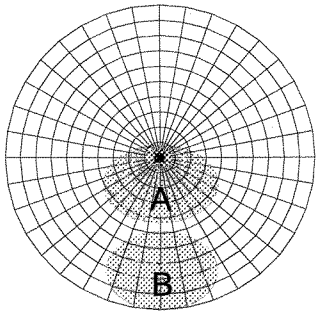

D. Fuel/Air Ratio Patterns.

Figure 2. Grid Characteristics for KIVA-II Analyses of Integrated Mixer-Flame Holder.

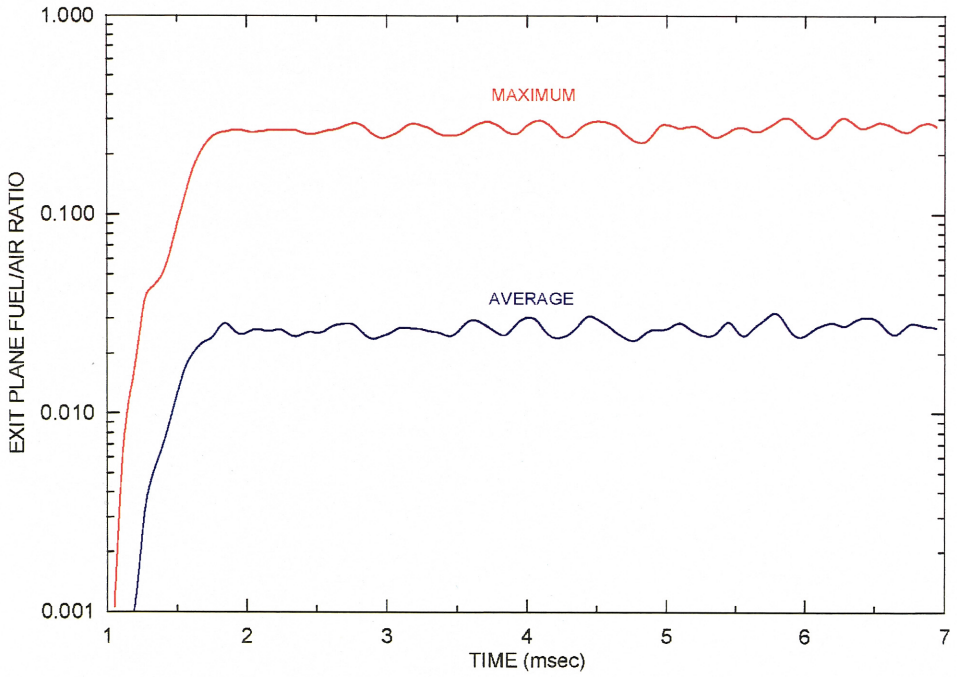

Figure 3. Average and Maximum Exit Plane Fuel/Air Ratio Time Histories (Baseline Case).

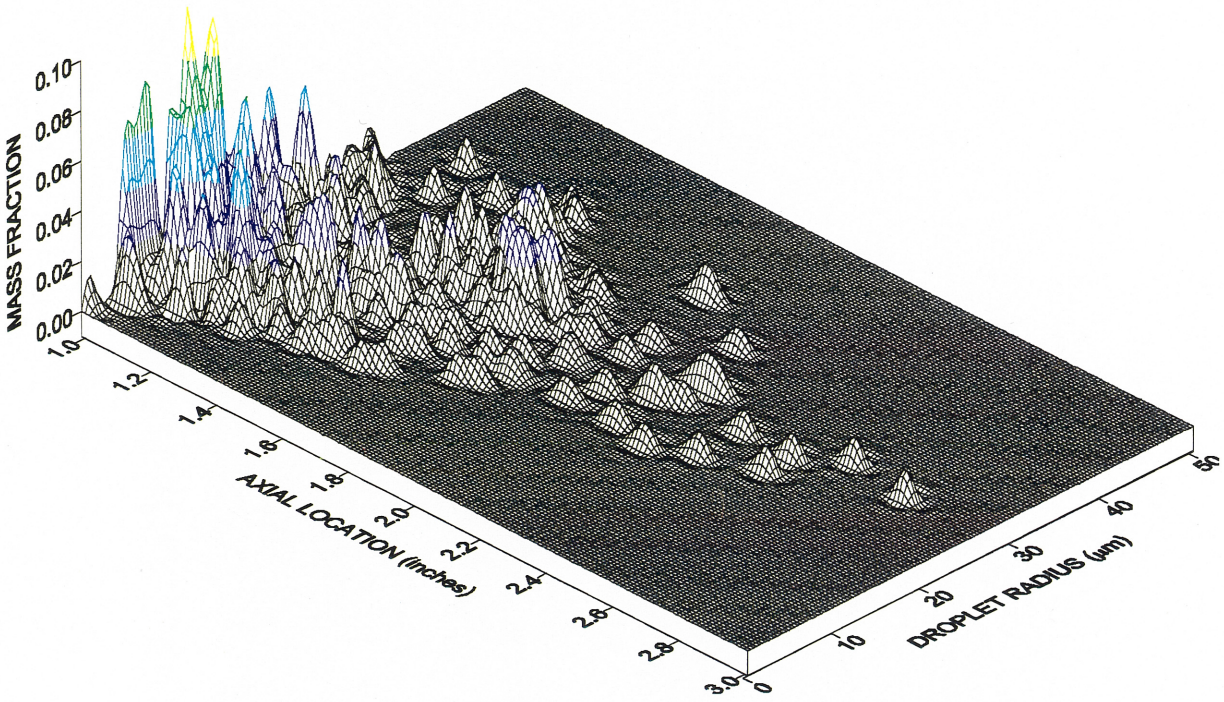

Figure 4. Fuel Droplet Distribution at 2 msec (Baseline Case).

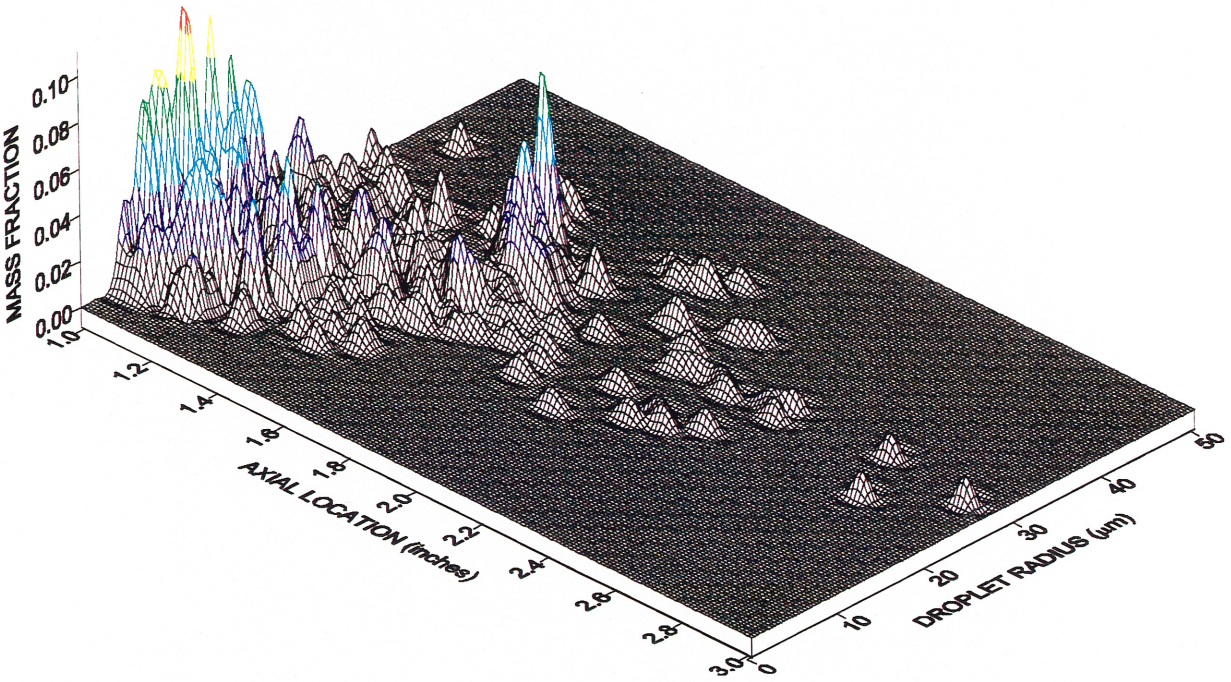

Figure 5. Fuel Droplet Distribution at 4 msec (Baseline Case).

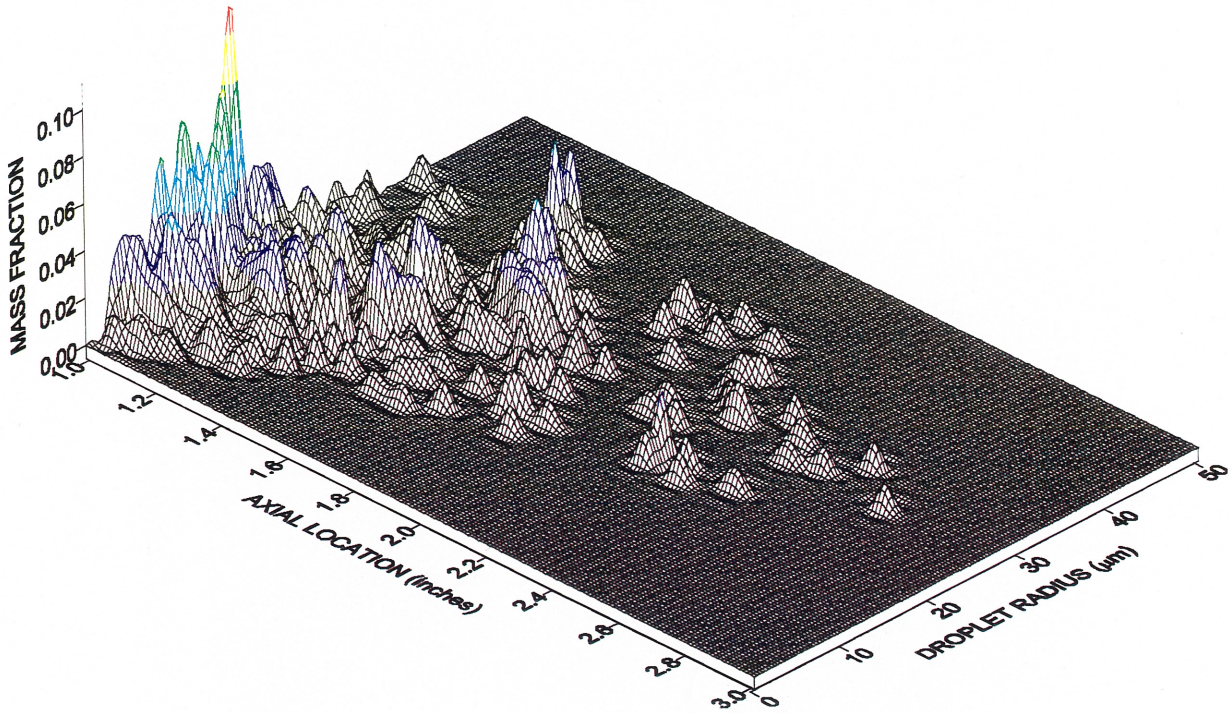

Figure 6. Fuel Droplet Distribution at 6 msec (Baseline Case).

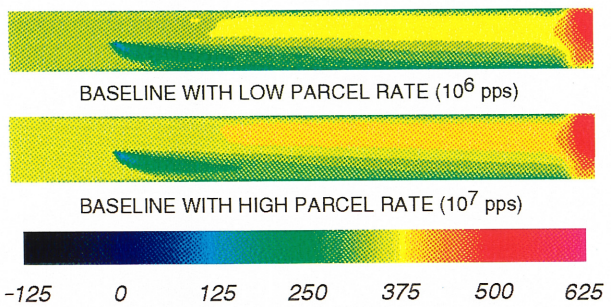

A. Axial Velocity (fps).

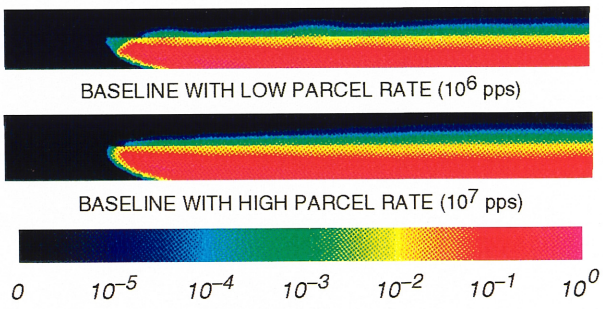

B. Fuel/Air Ratio.

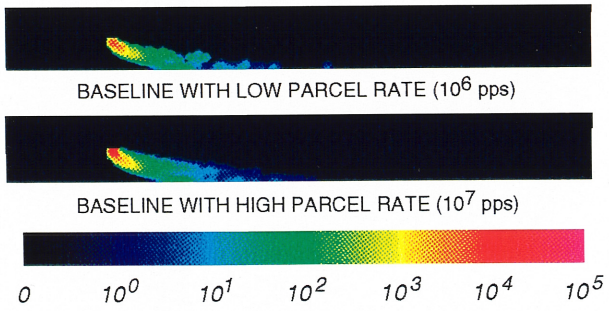

C. Fuel Droplet Population.

f/a_{min}	$f/a_{avg} \times 10^{-2}$	$f/a_{max} \times 10^{-1}$
BASELINE WITH LOW PARCEL RATE (10^6 pps)		
2.1597×10^{-8}	2.6903	2.7039
BASELINE WITH HIGH PARCEL RATE (10^7 pps)		
3.7550×10^{-8}	2.7105	2.6670

D. Exit Plane Fuel/Air Ratio.

Figure 7. Baseline Cases with Varying Injection Rates of Computational Droplet Parcels.

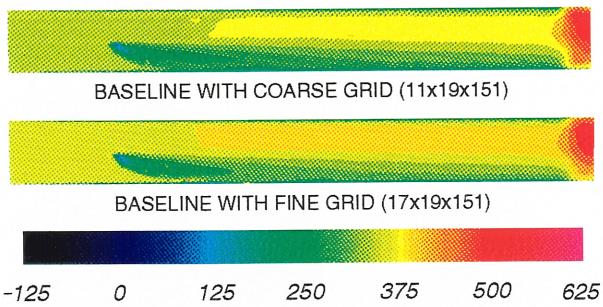

A. Axial Velocity (fps).

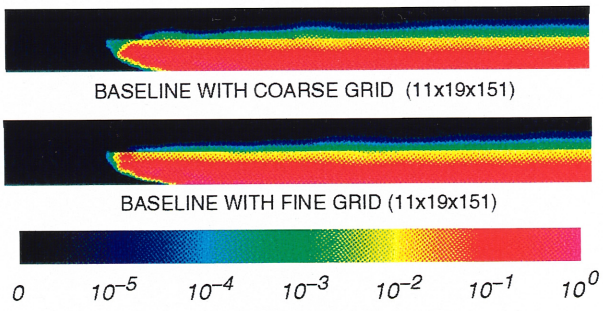

B. Fuel/Air Ratio.

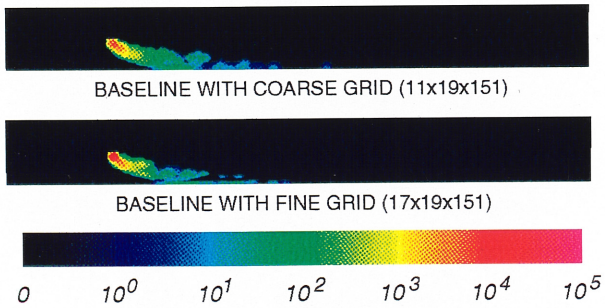

C. Fuel Droplet Population.

f/a_{min}	$f/a_{avg} \times 10^{-2}$	$f/a_{max} \times 10^{-1}$
BASELINE WITH COARSE GRID (11x19x151)		
2.1597×10^{-8}	2.6903	2.7039
BASELINE WITH FINE GRID (17x19x151)		
5.8447×10^{-8}	2.8918	2.7209

Figure 8. Baseline Cases with Coarse and Fine Grids.

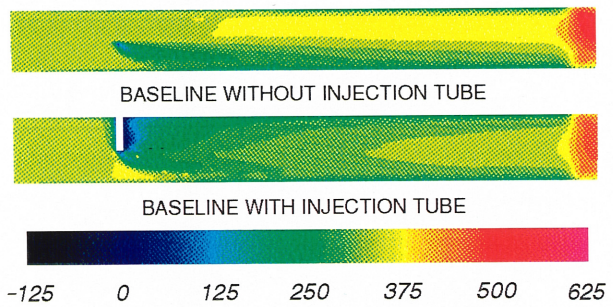

A. Axial Velocity (fps).

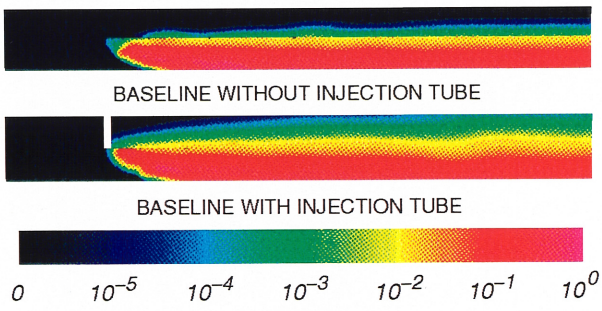

B. Fuel/Air Ratio.

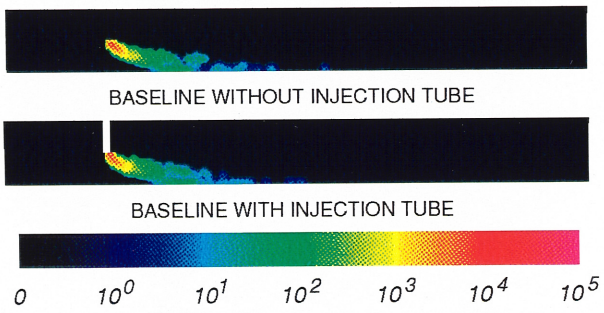

C. Fuel Droplet Population.

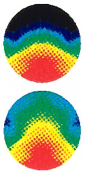

f/a_{min}	$f/a_{avg} \times 10^{-2}$	$f/a_{max} \times 10^{-1}$
BASELINE WITHOUT INJECTION TUBE		
2.1597×10^{-8}	2.6903	2.7039
BASELINE WITH INJECTION TUBE		
3.7385×10^{-5}	2.9617	2.4949

D. Exit Plane Fuel/Air Ratio.

Figure 9. Baseline Cases with and without Injection Tube.

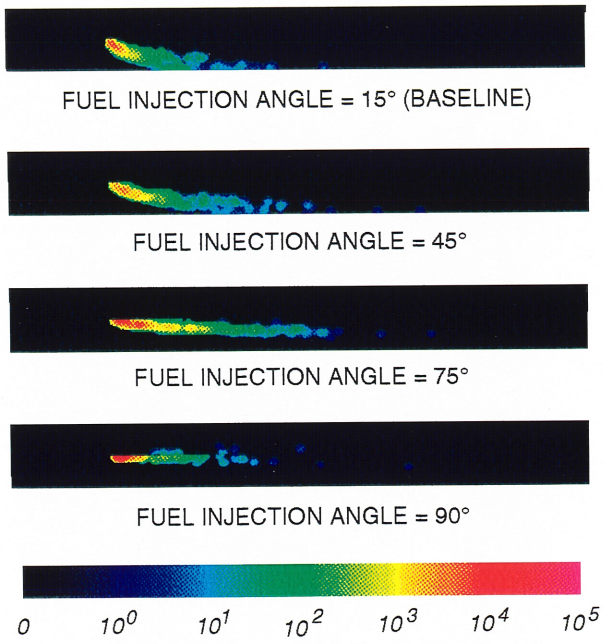

A. Fuel Droplet Population.

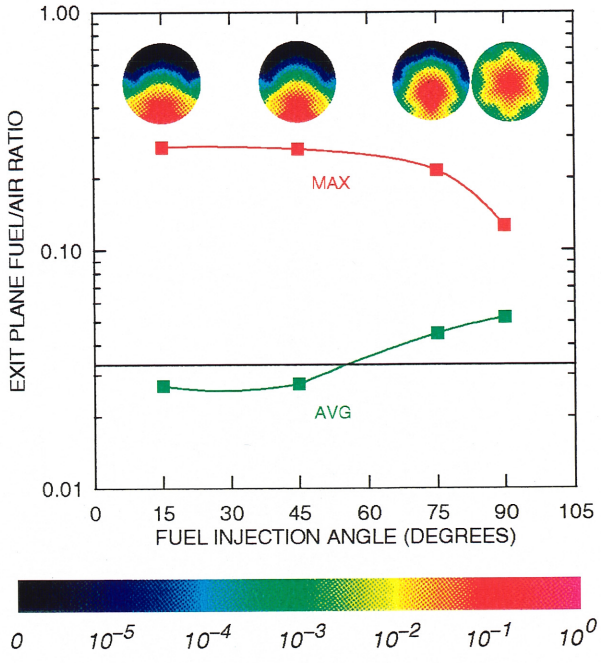

B. Exit Plane Fuel/Air Ratio.

Figure 10. Fuel Injection Angle Effects.

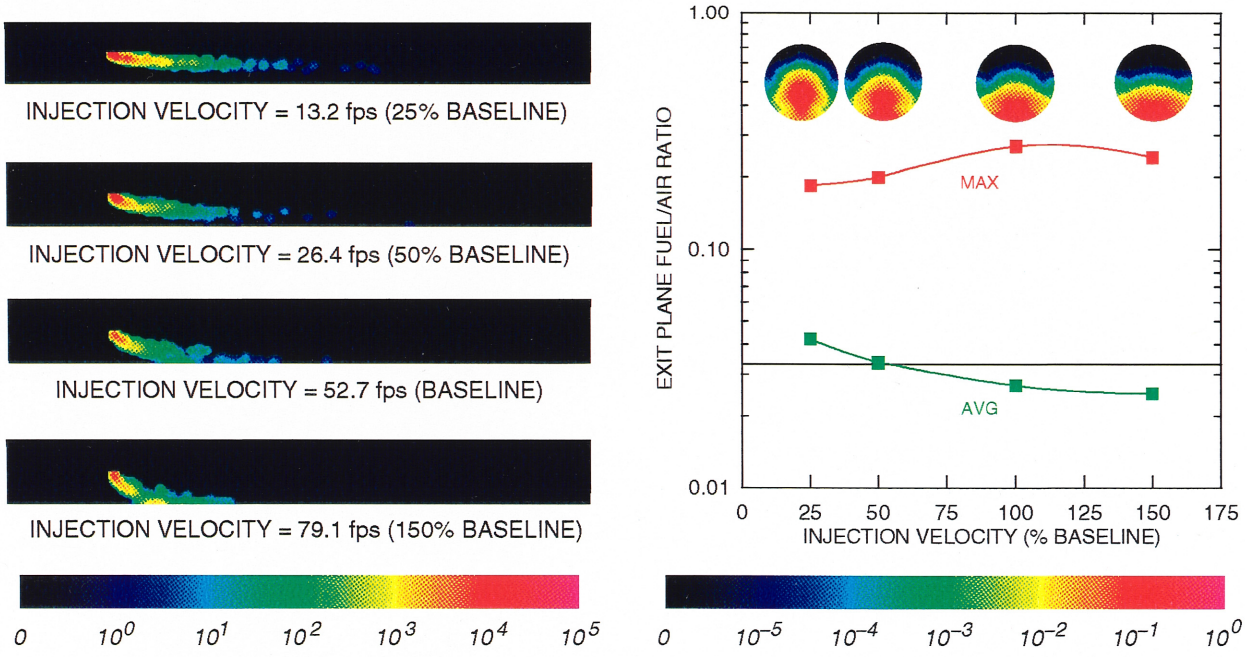

A. Fuel Droplet Population.

B. Exit Plane Fuel/Air Ratio.

Figure 11. Fuel Injection Velocity Effects.

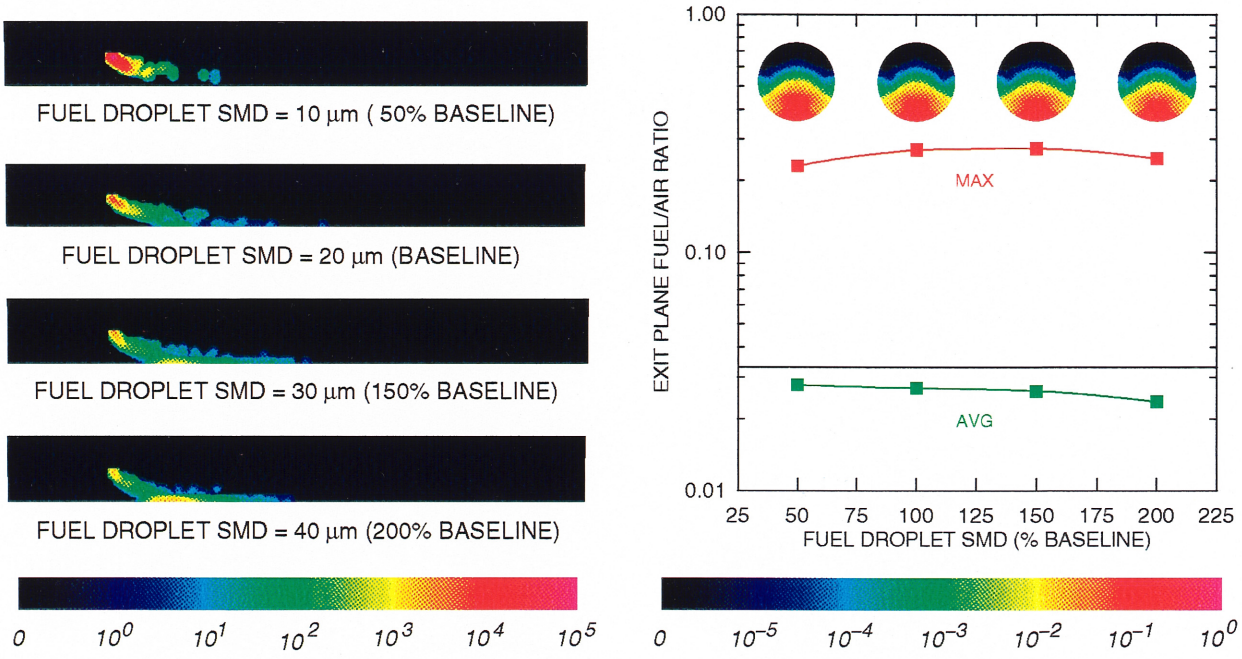

A. Fuel Droplet Population.

B. Exit Plane Fuel/Air Ratio.

Figure 12. Fuel Droplet SMD Effects.

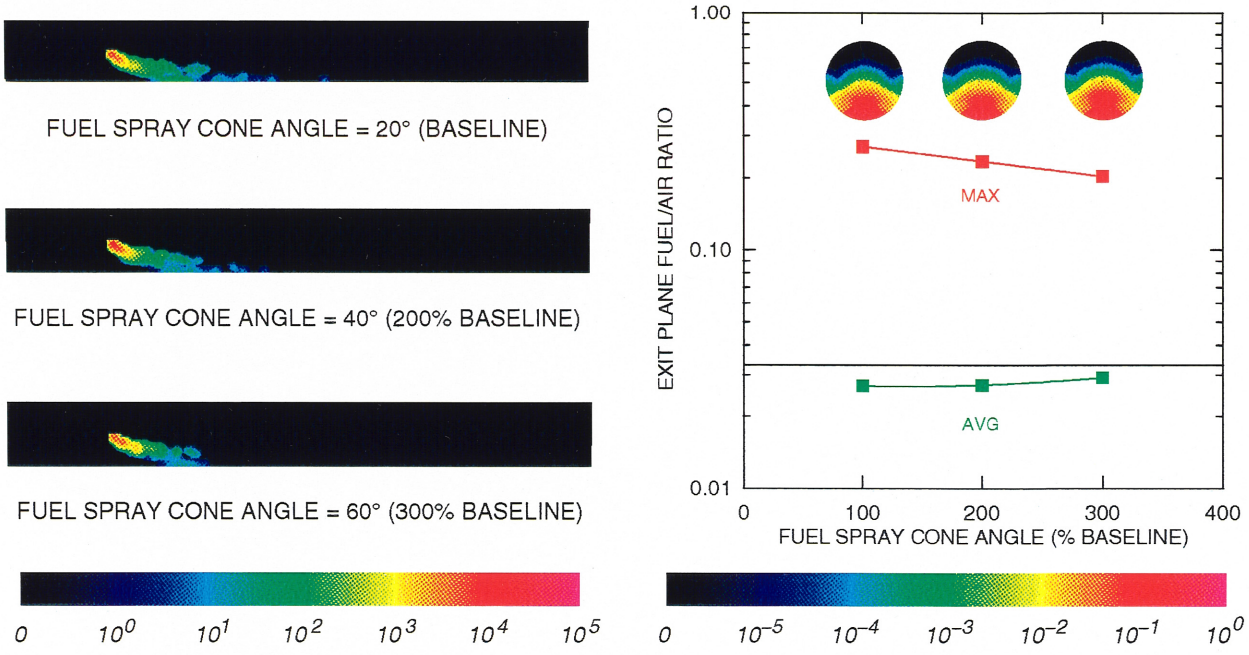

A. Fuel Droplet Population.

B. Exit Plane Fuel/Air Ratio.

Figure 13. Fuel Spray Cone Angle Effects.

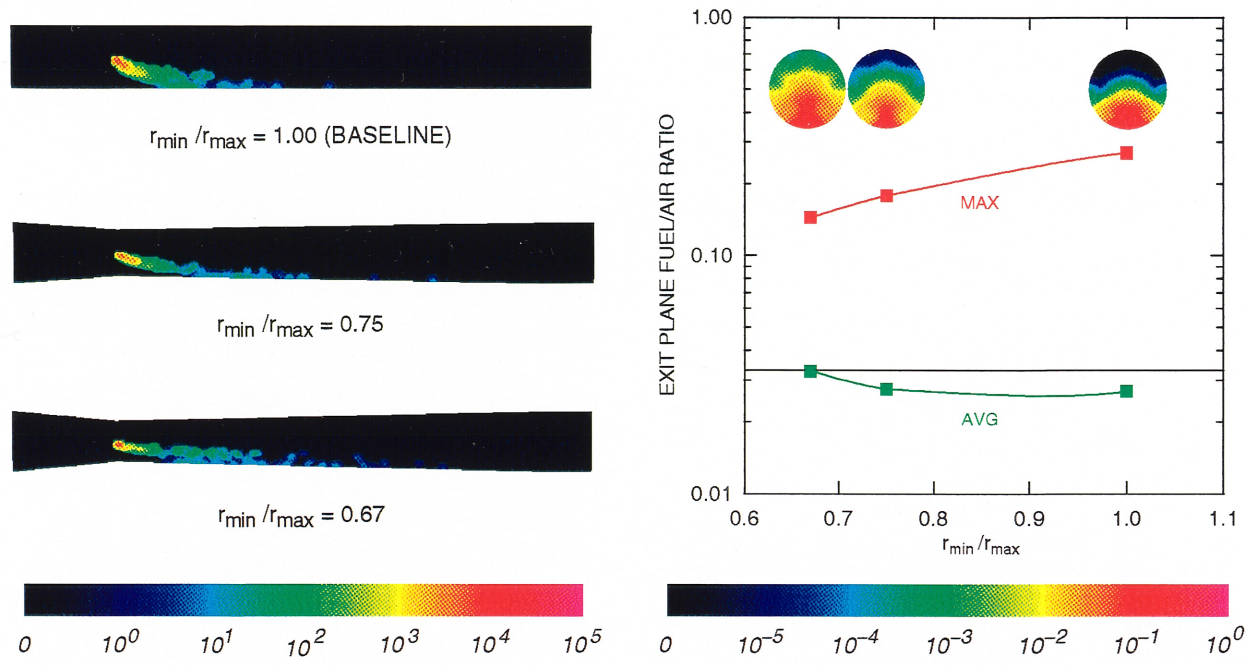

A. Fuel Droplet Population.

B. Exit Plane Fuel/Air Ratio.

Figure 14. Venturi Tube Effects.

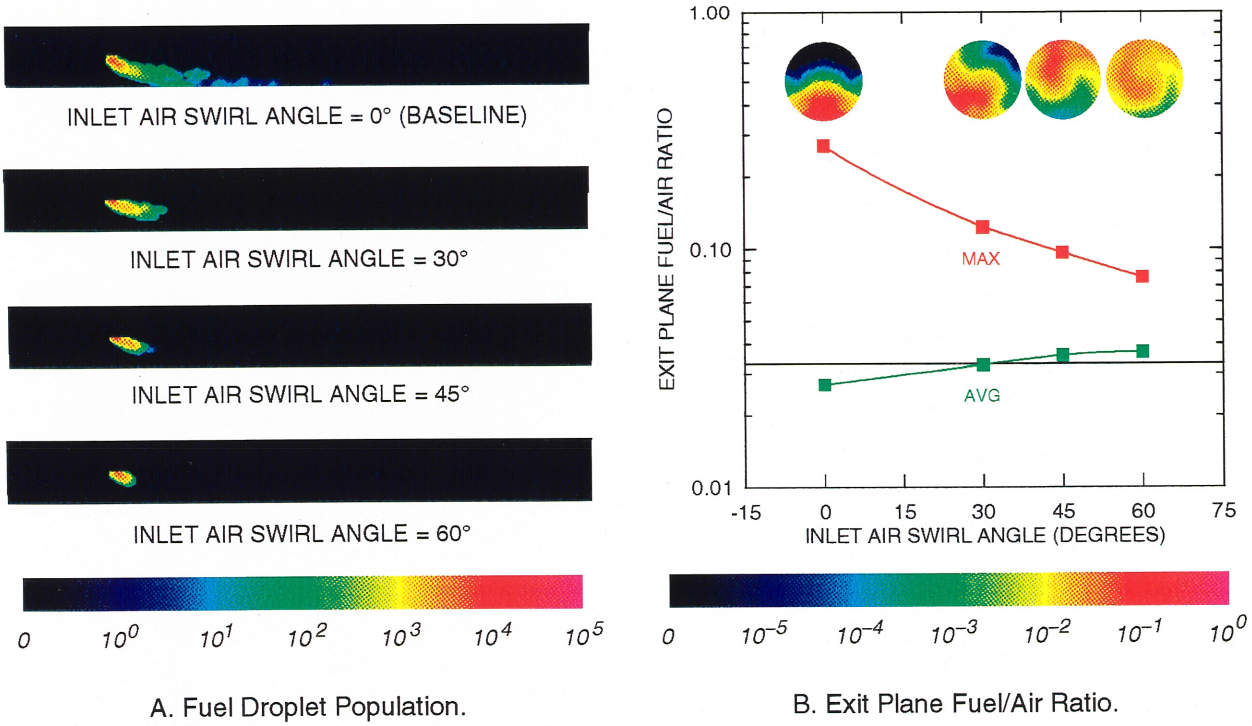

A. Fuel Droplet Population.

B. Exit Plane Fuel/Air Ratio.

Figure 15. Inlet Air Swirl Angle Effects.

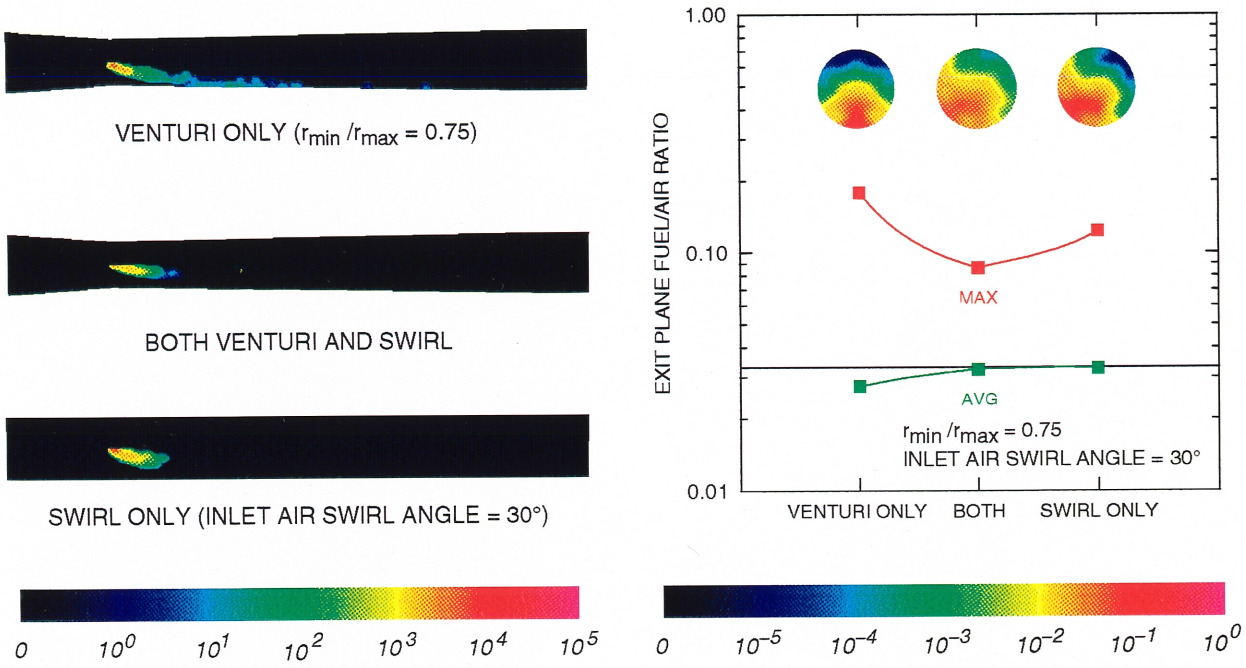

A. Fuel Droplet Population.

B. Exit Plane Fuel/Air Ratio.

Figure 16. Combined Venturi and Inlet Air Swirl Angle Effects.

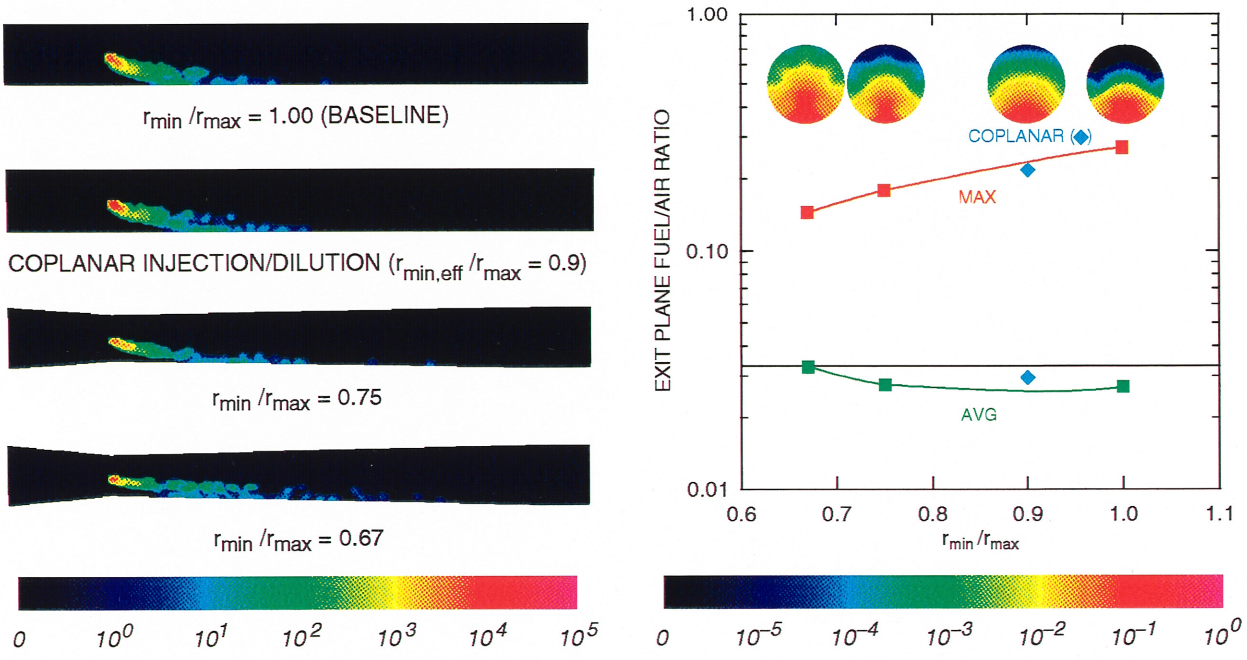

A. Fuel Droplet Population.

B. Exit Plane Fuel/Air Ratio.

Figure 17. Coplanar Injection/Dilution Effects.

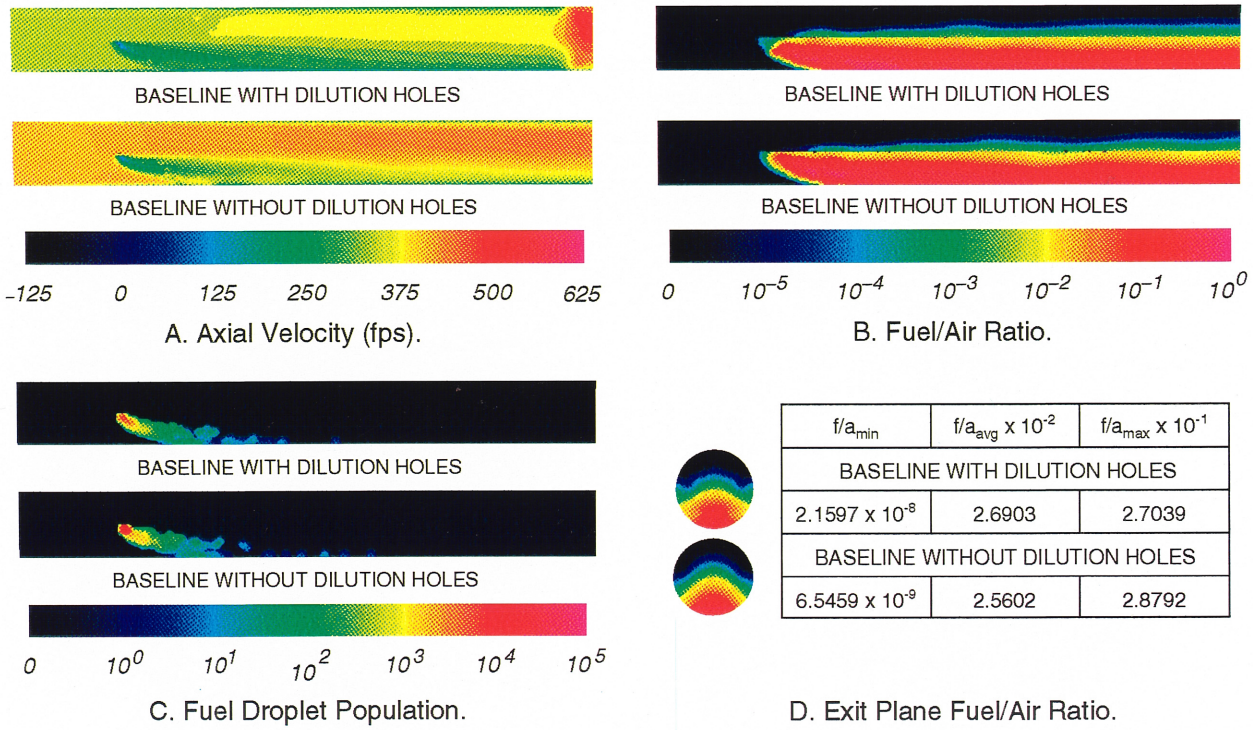

A. Axial Velocity (fps).

B. Fuel/Air Ratio.

C. Fuel Droplet Population.

f/a_{min}	$f/a_{avg} \times 10^{-2}$	$f/a_{max} \times 10^{-1}$
BASELINE WITH DILUTION HOLES		
2.1597×10^{-8}	2.6903	2.7039
BASELINE WITHOUT DILUTION HOLES		
6.5459×10^{-9}	2.5602	2.8792

D. Exit Plane Fuel/Air Ratio.

Figure 18. Baseline Cases with and without Dilution Holes.

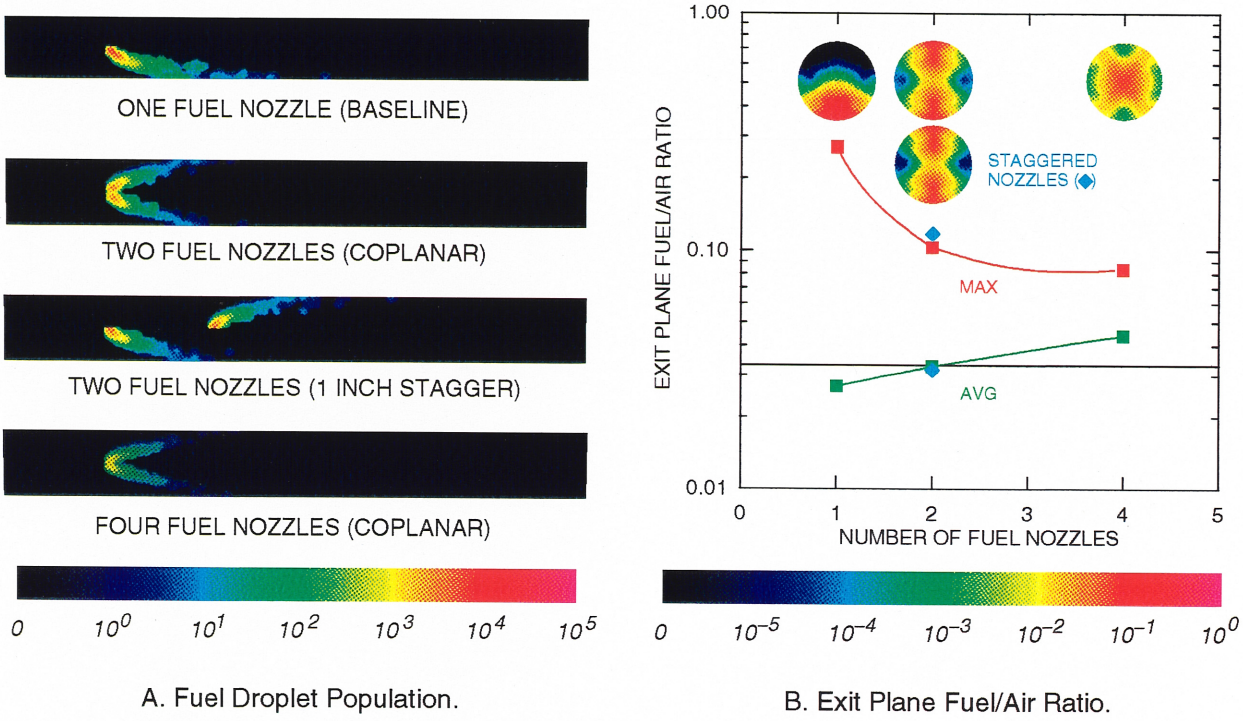

Figure 19. Multiple Fuel Nozzle Effects.

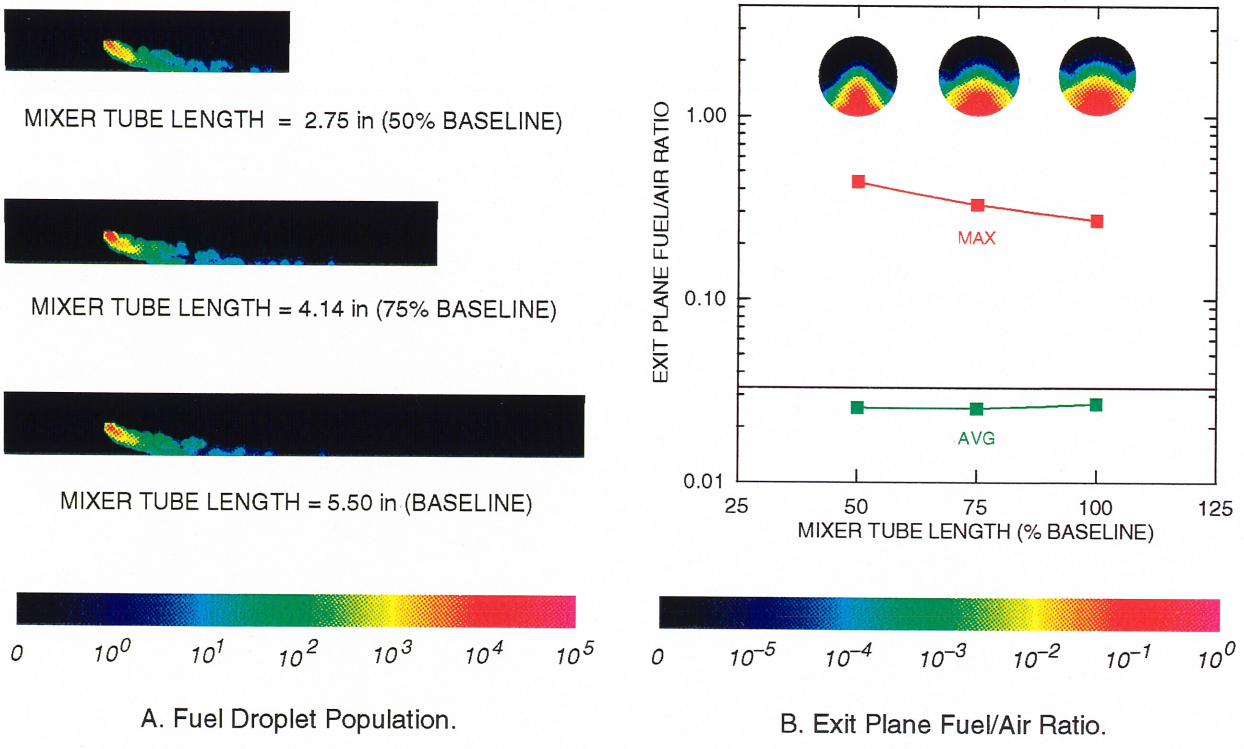

Figure 20. Mixer Tube Length Effects.

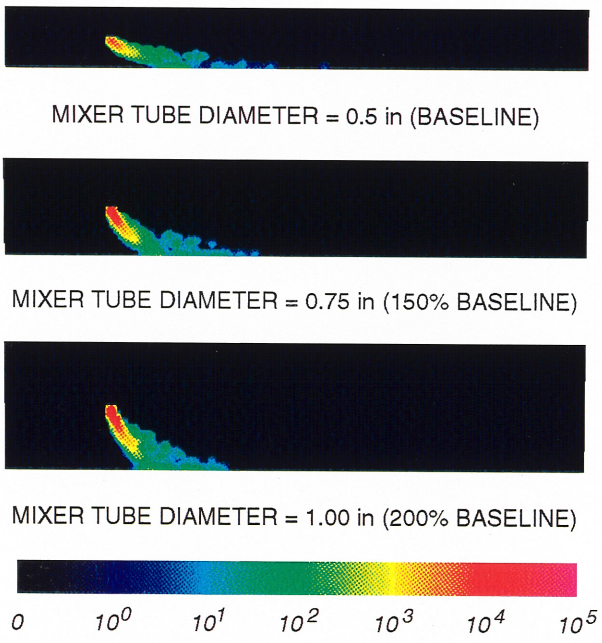

A. Fuel Droplet Population.

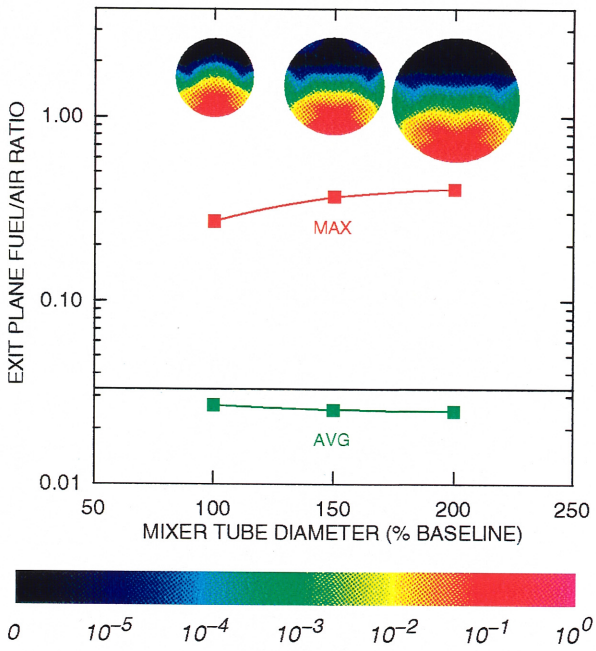

B. Exit Plane Fuel/Air Ratio.

Figure 21. Mixer Tube Diameter Effects ($\mathring{m}_{air}$ = constant).

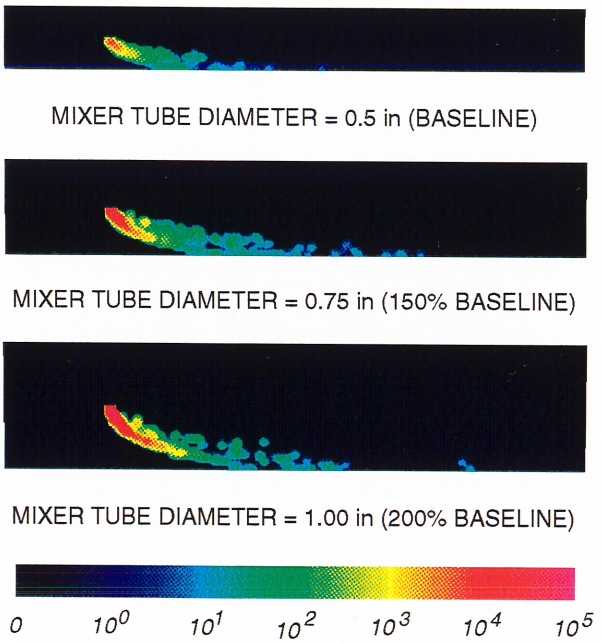

A. Fuel Droplet Population.

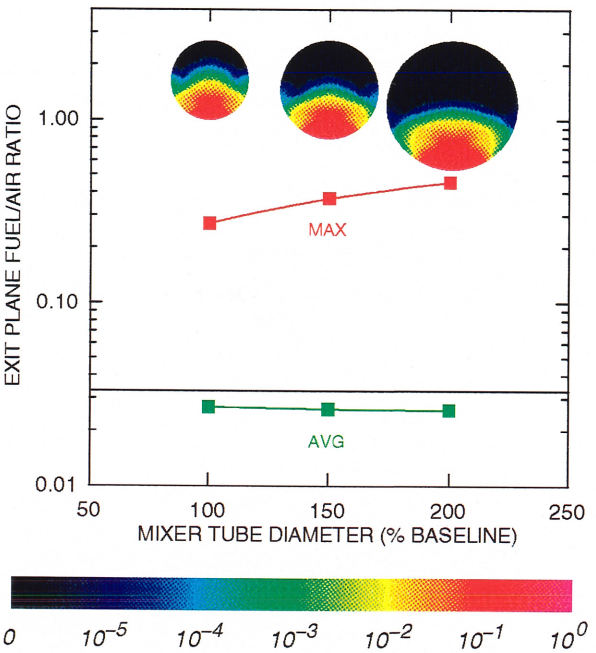

B. Exit Plane Fuel/Air Ratio.

Figure 22. Mixer Tube Diameter Effects (v_{air} = constant, Baseline Air Flow Splits).

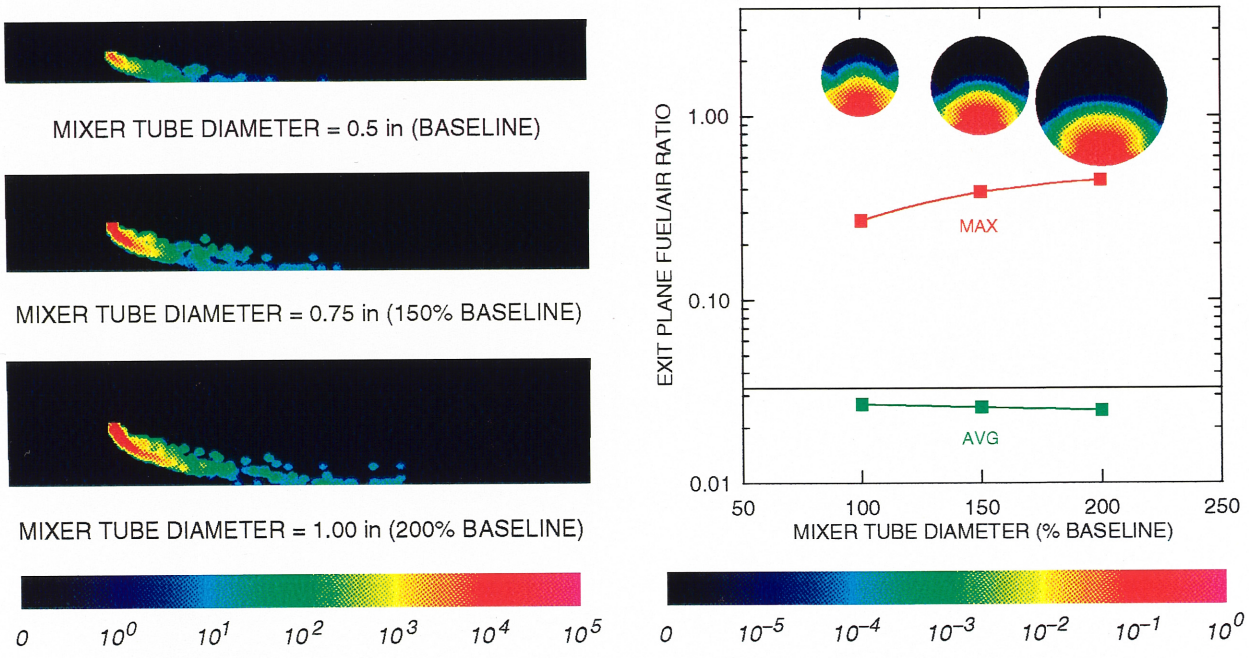

A. Fuel Droplet Population.

B. Exit Plane Fuel/Air Ratio.

Figure 23. Mixer Tube Diameter Effects (v_{air} = constant, Baseline Dilution Flow).

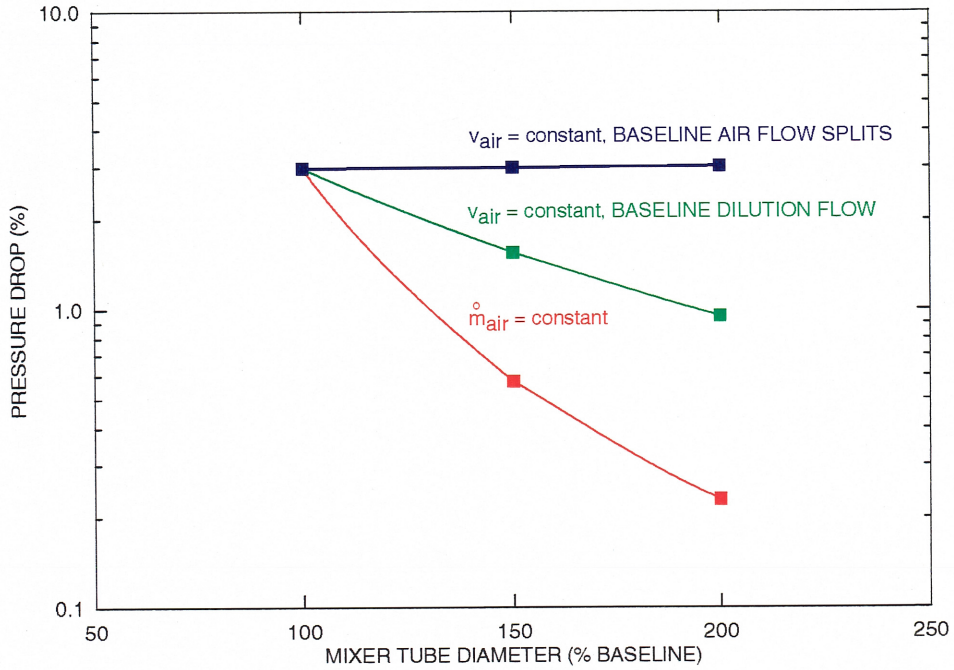

Figure 24. Mixer Tube Diameter Effects: Pressure Drops (without Dump).

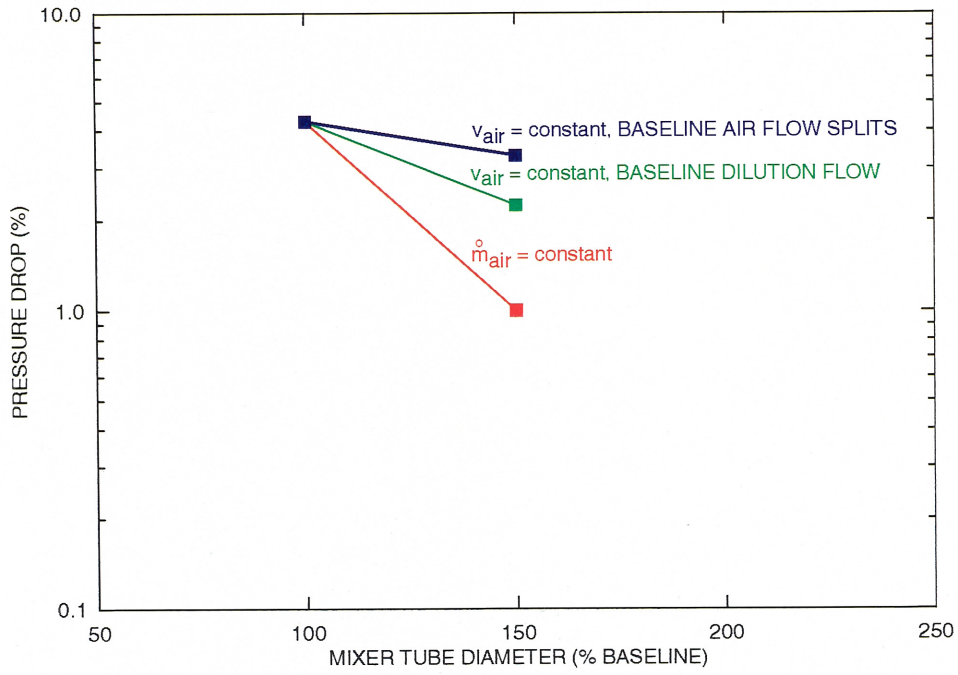

Figure 25. Mixer Tube Diameter Effects: Pressure Drops (with Dump).

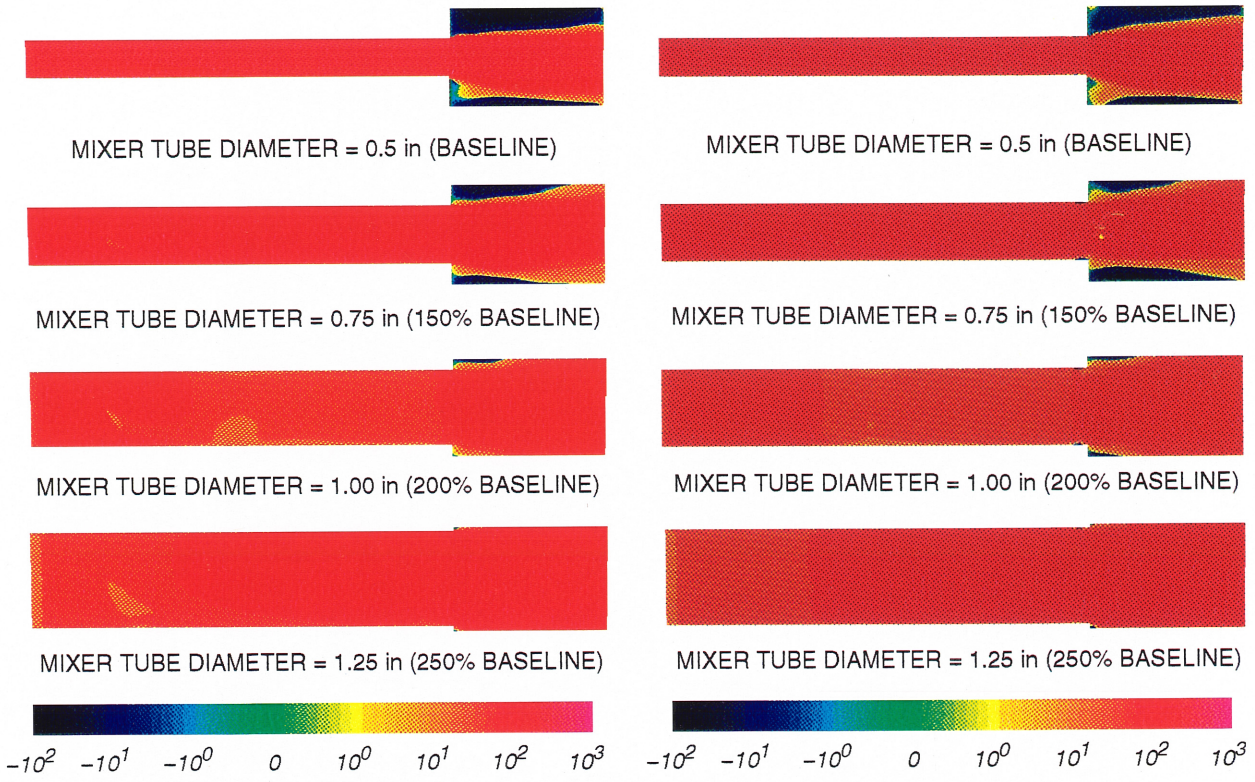

A. Axial Velocity in Fuel Injection Plane (fps).

B. Axial Velocity in Fuel Injection Plane + 45° (fps).

Figure 26. Mixer Tube Diameter Effects ($\dot{m}_{air}$ = constant): Combustion Results.

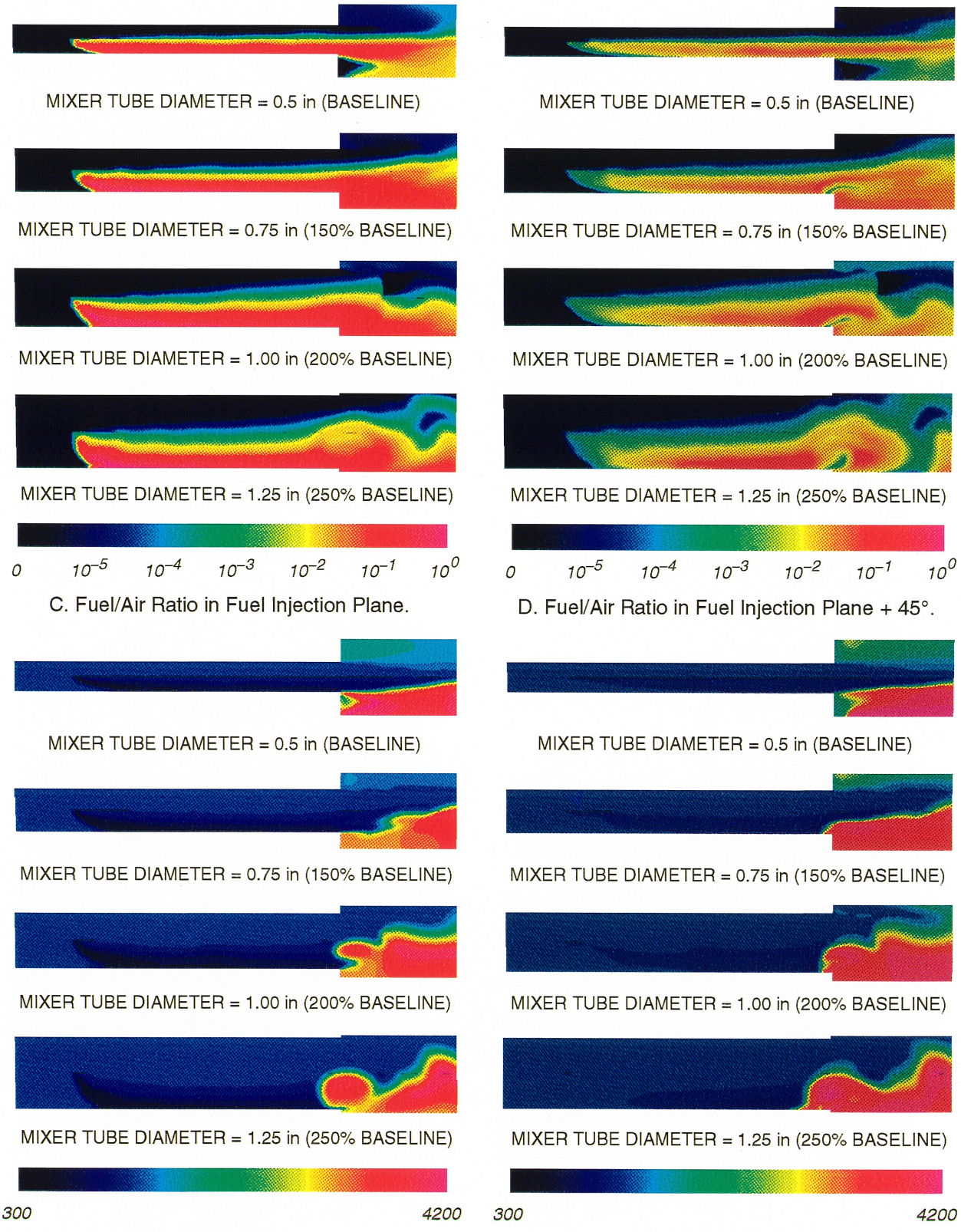

C. Fuel/Air Ratio in Fuel Injection Plane.

D. Fuel/Air Ratio in Fuel Injection Plane + 45°.

E. Temperature in Fuel Injection Plane (° F).

F. Temperature in Fuel Injection Plane + 45° (° F).

Figure 26. Mixer Tube Diameter Effects ($\dot{m}_{air}$ = constant): Combustion Results (Continued).

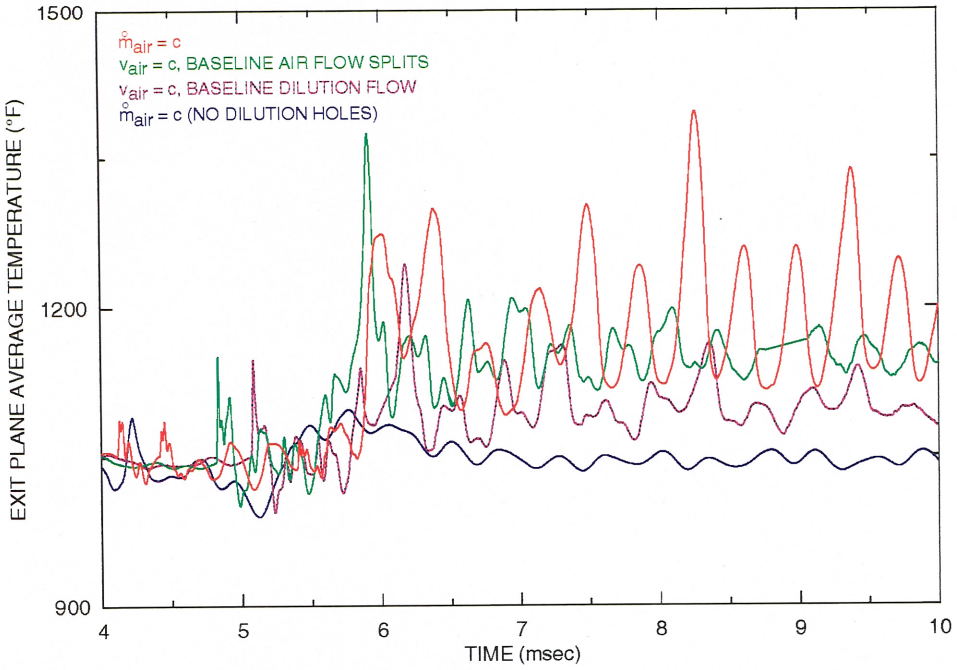

A. Exit Plane Average Temperature Time Histories.

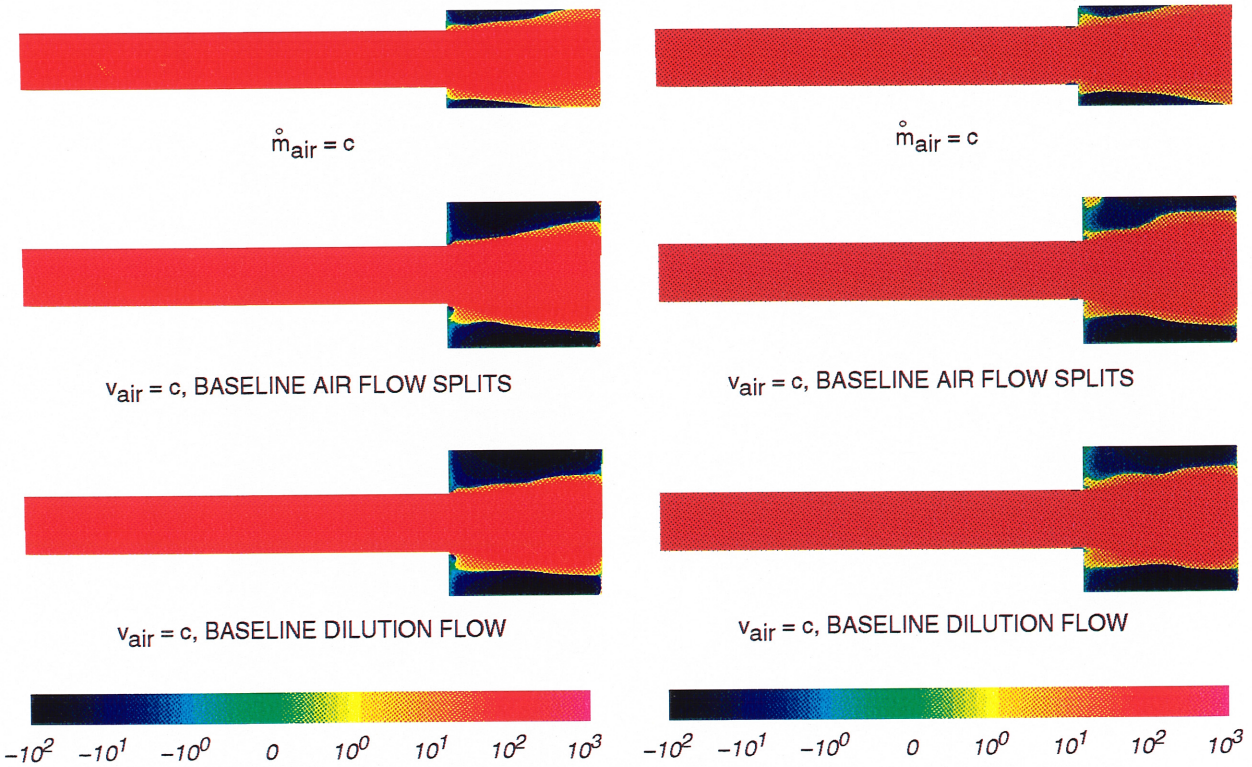

B. Axial Velocity in Fuel Injection Plane (fps).

C. Axial Velocity in Fuel Injection Plane + 45° (fps).

Figure 27. Flashback in 150% Baseline Diameter Mixer Tube.

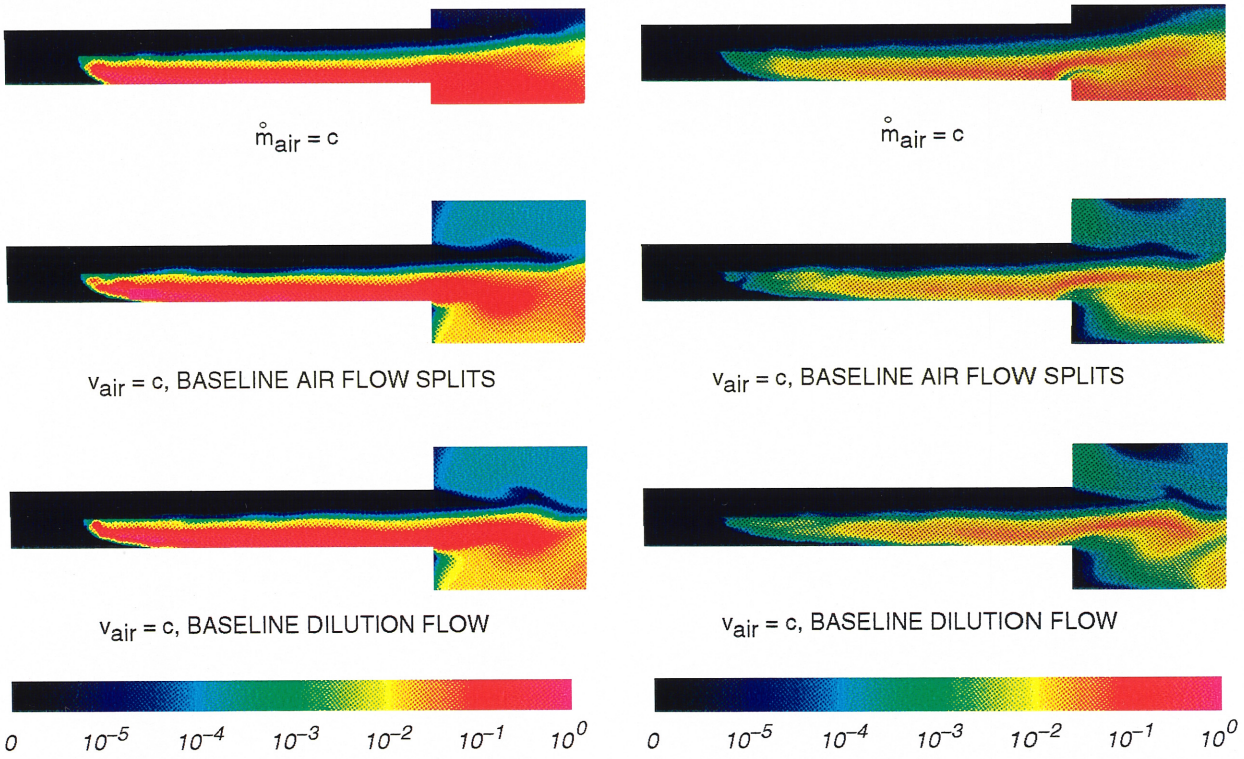

D. Fuel/Air Ratio in Fuel Injection Plane.

E. Fuel/Air Ratio in Fuel Injection Plane + 45°.

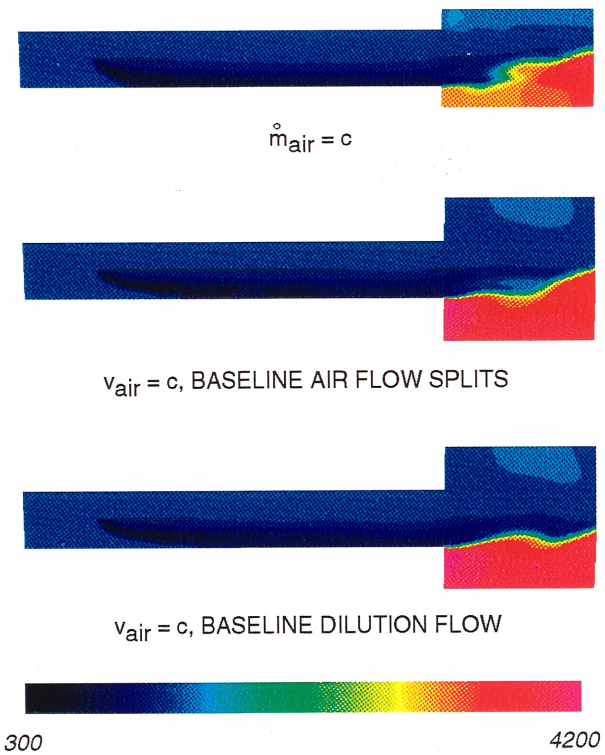

F. Temperature in Fuel Injection Plane (° F).

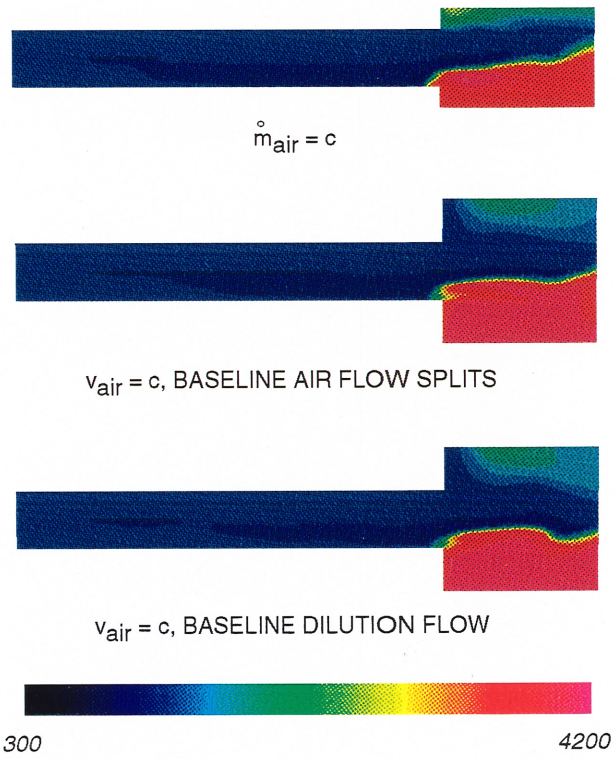

G. Temperature in Fuel Injection Plane + 45° (° F).

Figure 27. Flashback in 150% Baseline Diameter Mixer Tube (Continued).

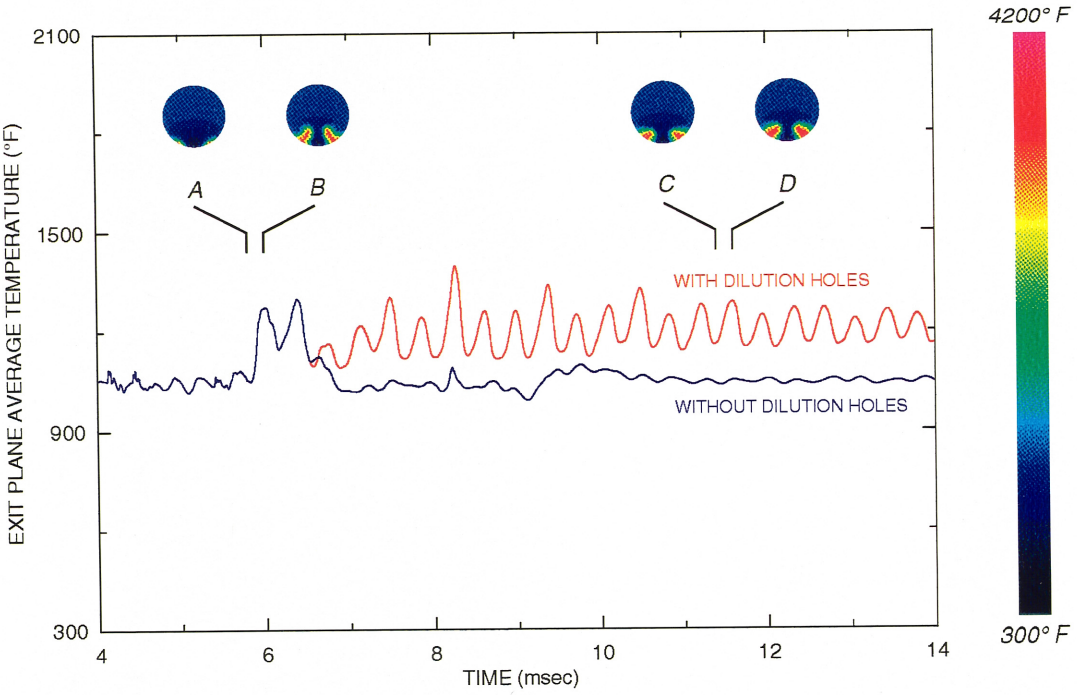

A. Exit Plane Average Temperature Time Histories.

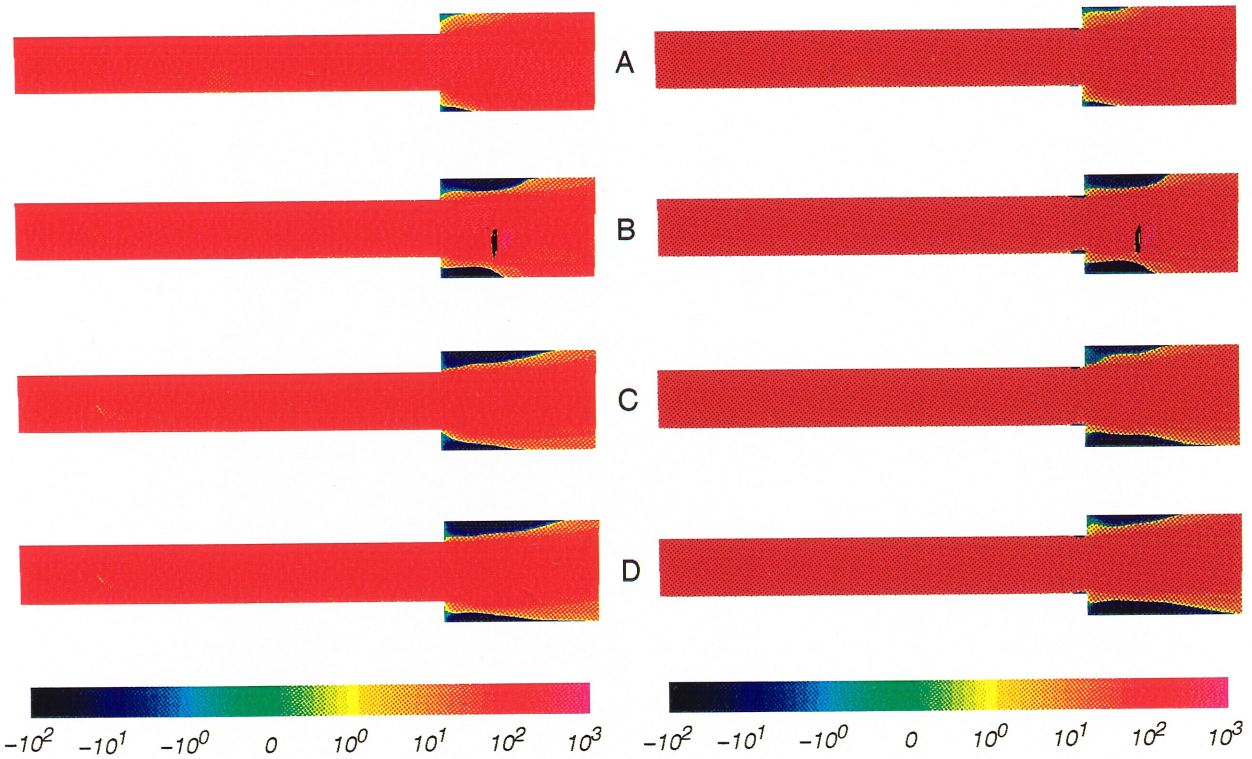

B. Axial Velocity in Fuel Injection Plane (fps).

C. Axial Velocity in Fuel Injection Plane + 45° (fps).

Figure 28. Flashback in 150% Baseline Diameter Mixer Tube ($\dot{m}_{air}$ = constant).

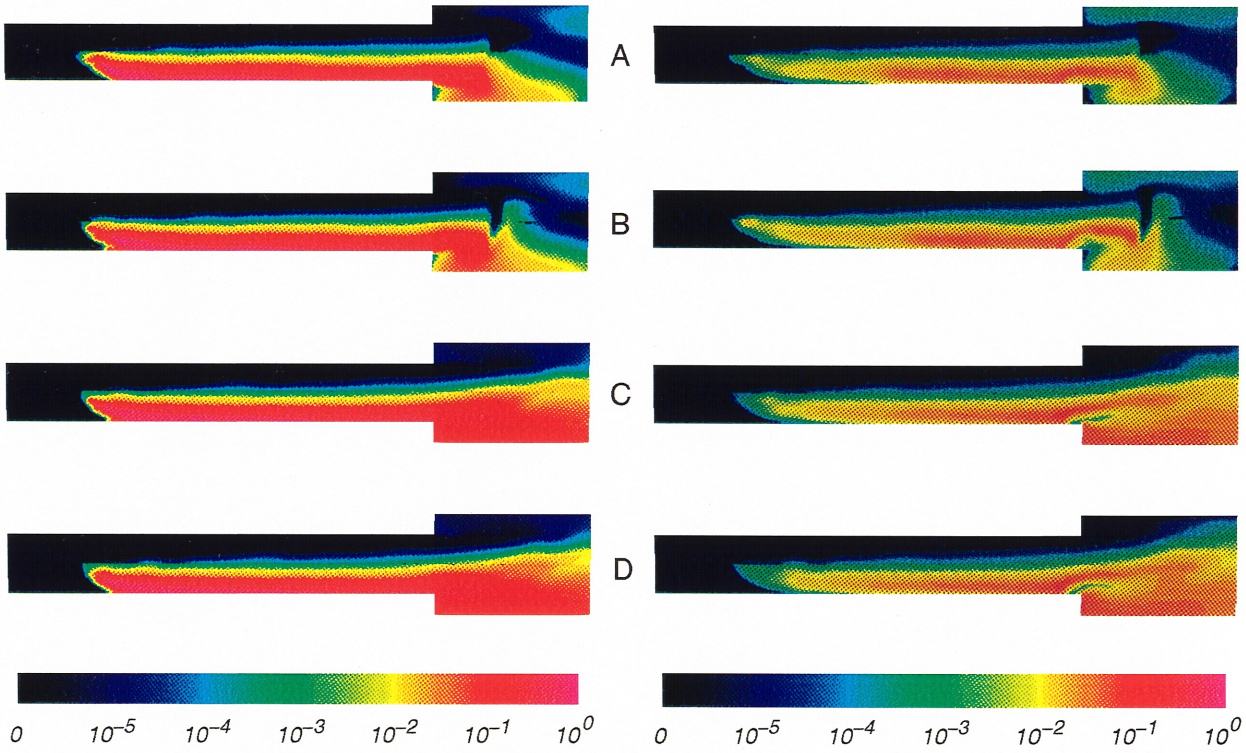

D. Fuel/Air Ratio in Fuel Injection Plane.

E. Fuel/Air Ratio in Fuel Injection Plane + 45°.

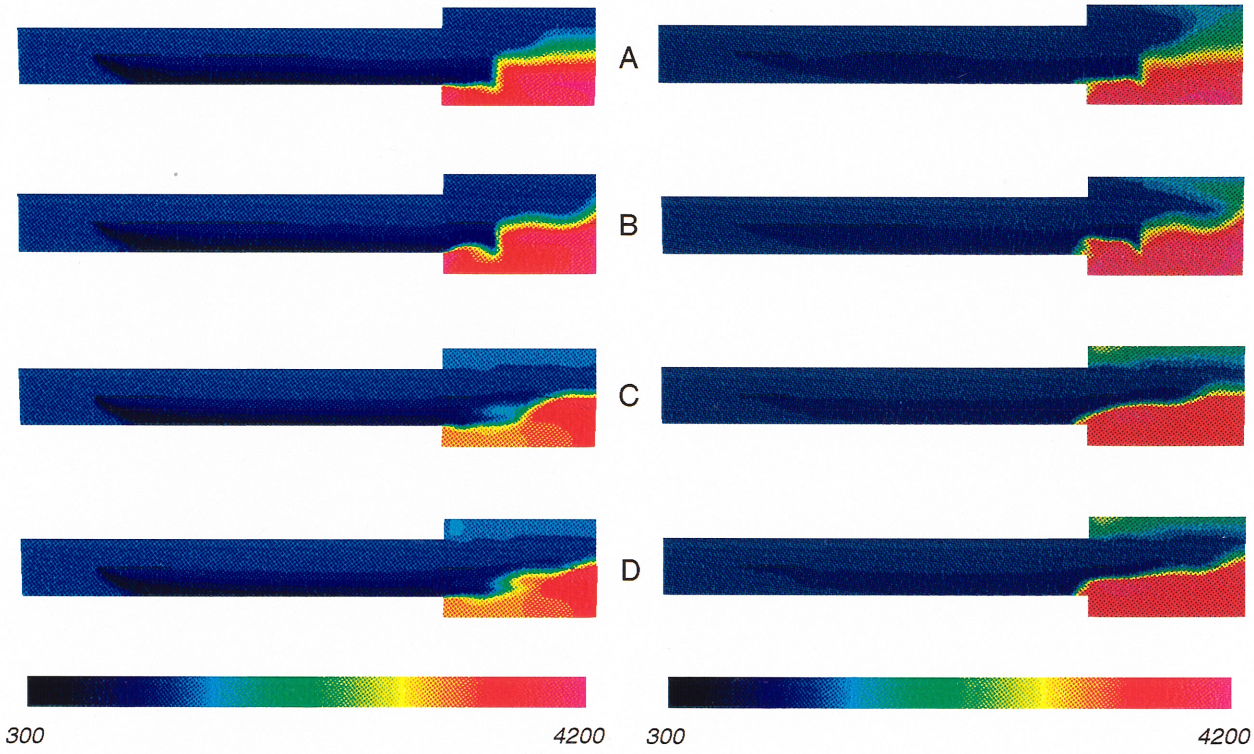

F. Temperature in Fuel Injection Plane (° F).

G. Temperature in Fuel Injection Plane + 45° (° F).

Figure 28. Flashback in 150% Baseline Diameter Mixer Tube ($\dot{m}_{air}$ = constant) (Continued).

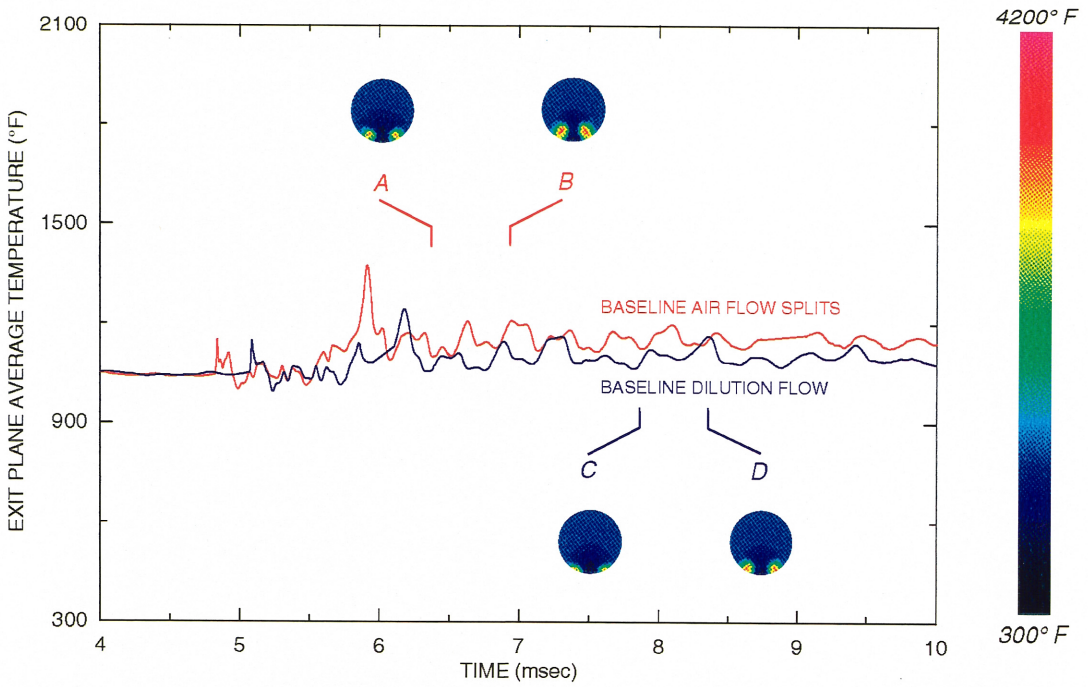

A. Exit Plane Average Temperature Time Histories.

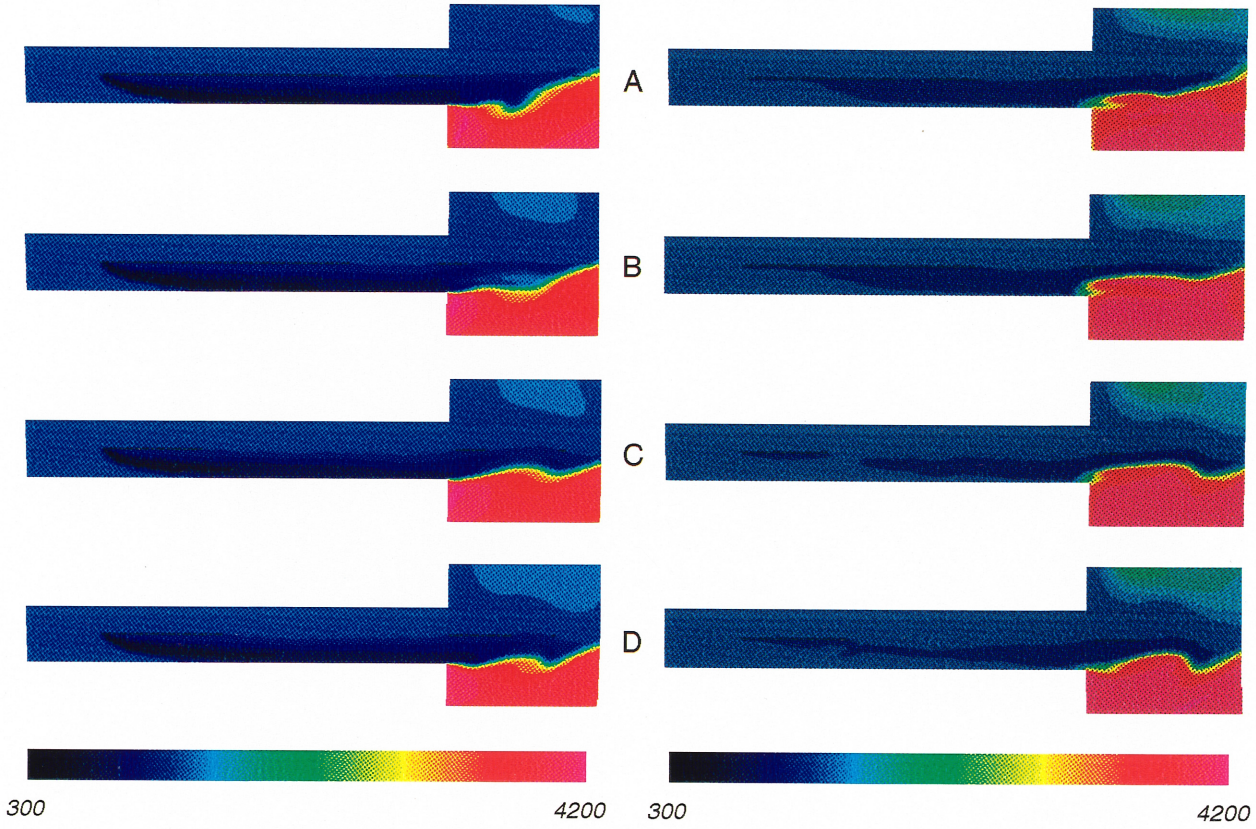

B. Temperature in Fuel Injection Plane (° F).

C. Temperature in Fuel Injection Plane + 45° (° F).

Figure 29. Flashback in 150% Baseline Diameter Mixer Tube (v_{air} = constant).

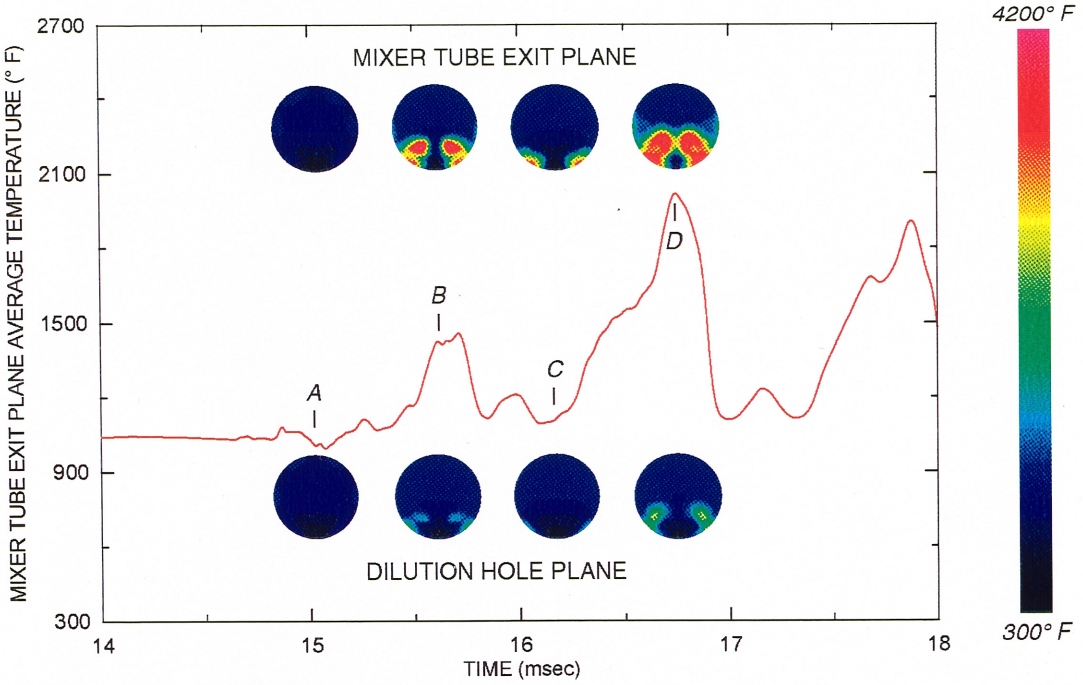

A. Exit Plane Average Temperature Time History.

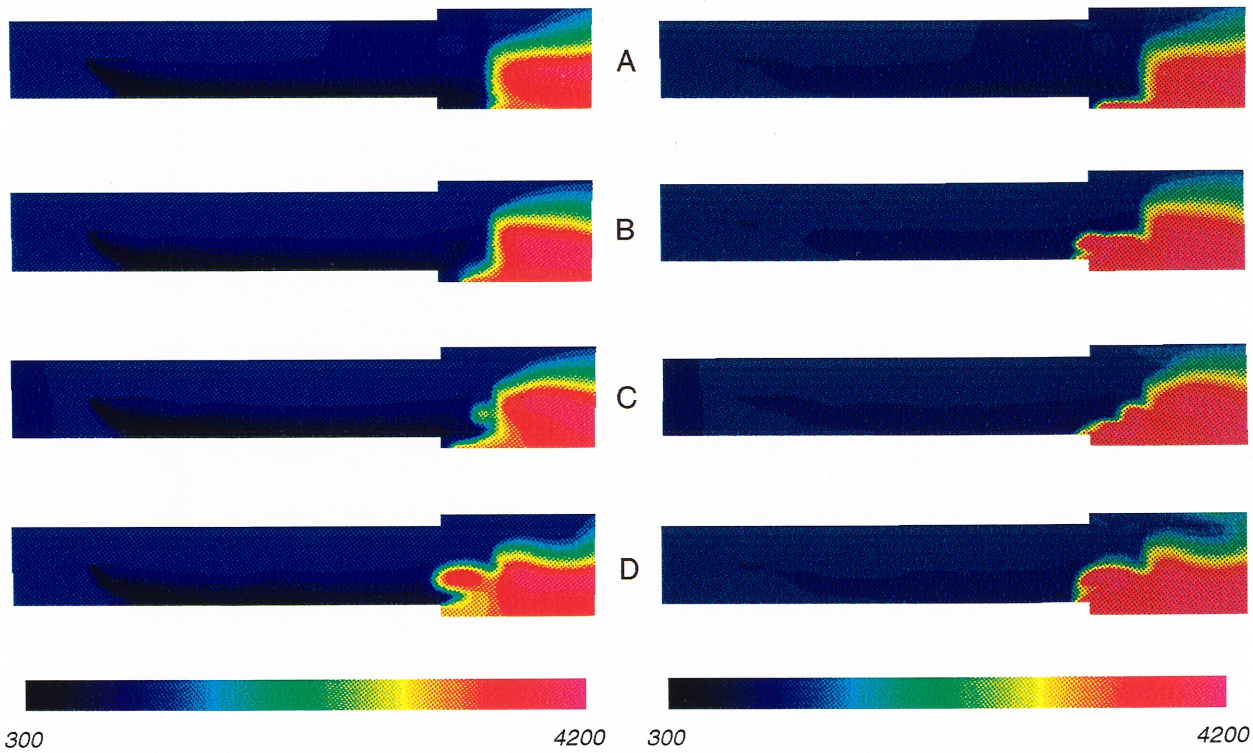

B. Temperature in Fuel Injection Plane (° F).

C. Temperature in Fuel Injection Plane + 45° (° F).

Figure 30. Flashback in 200% Baseline Diameter Mixer Tube ($\dot{m}_{air}$ = constant).

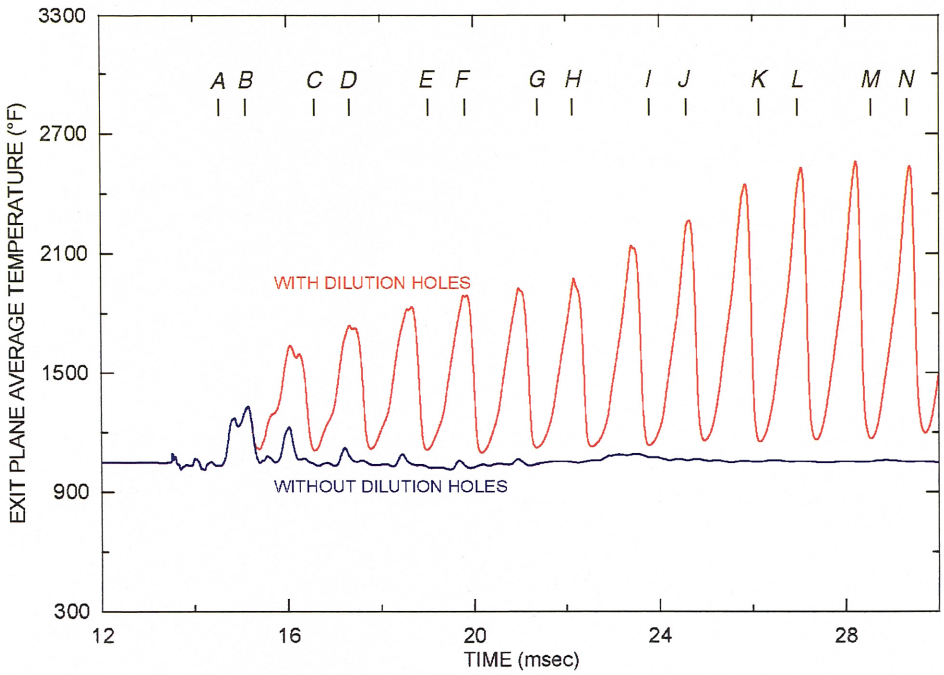

A. Exit Plane Average Temperature Time Histories.

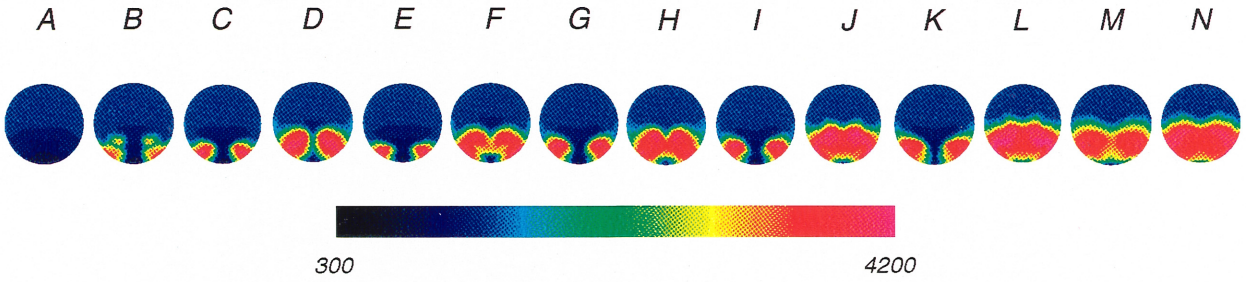

B. Exit Plane Temperature (° F).

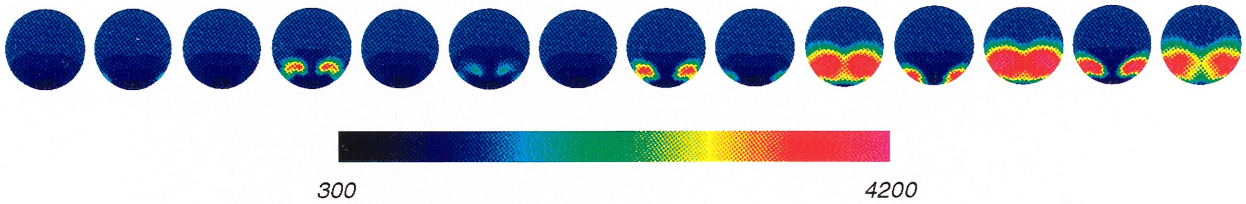

C. Dilution Hole Plane Temperature (° F).

Figure 31. Flashback in 250% Baseline Diameter Mixer Tube ($\dot{m}_{air}$ = constant).

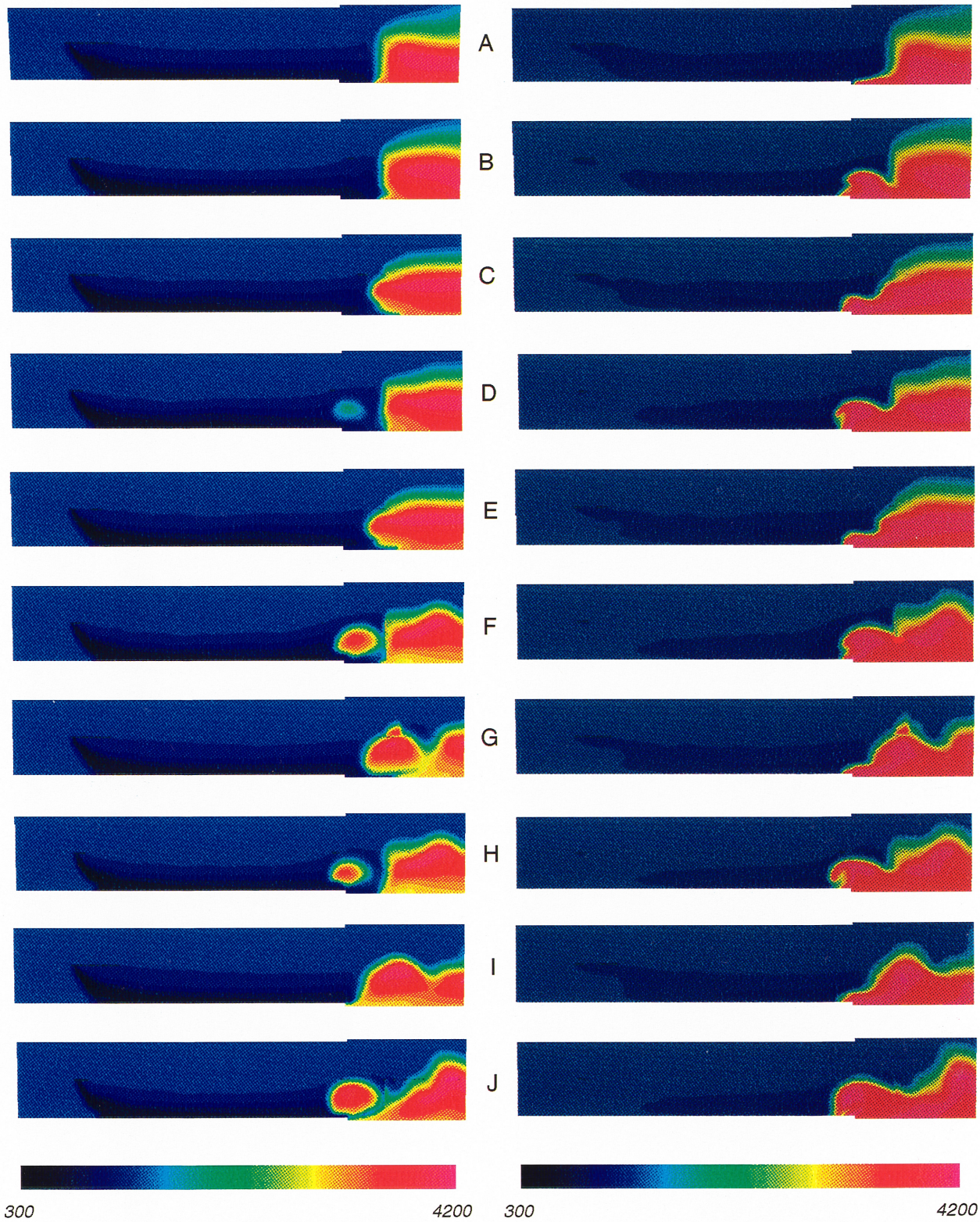

D. Temperature in Fuel Injection Plane (° F).

E. Temperature in Fuel Injection Plane + 45° (° F).

Figure 31. Flashback in 250% Baseline Diameter Mixer Tube ($\dot{m}_{air}$ = constant) (Continued).

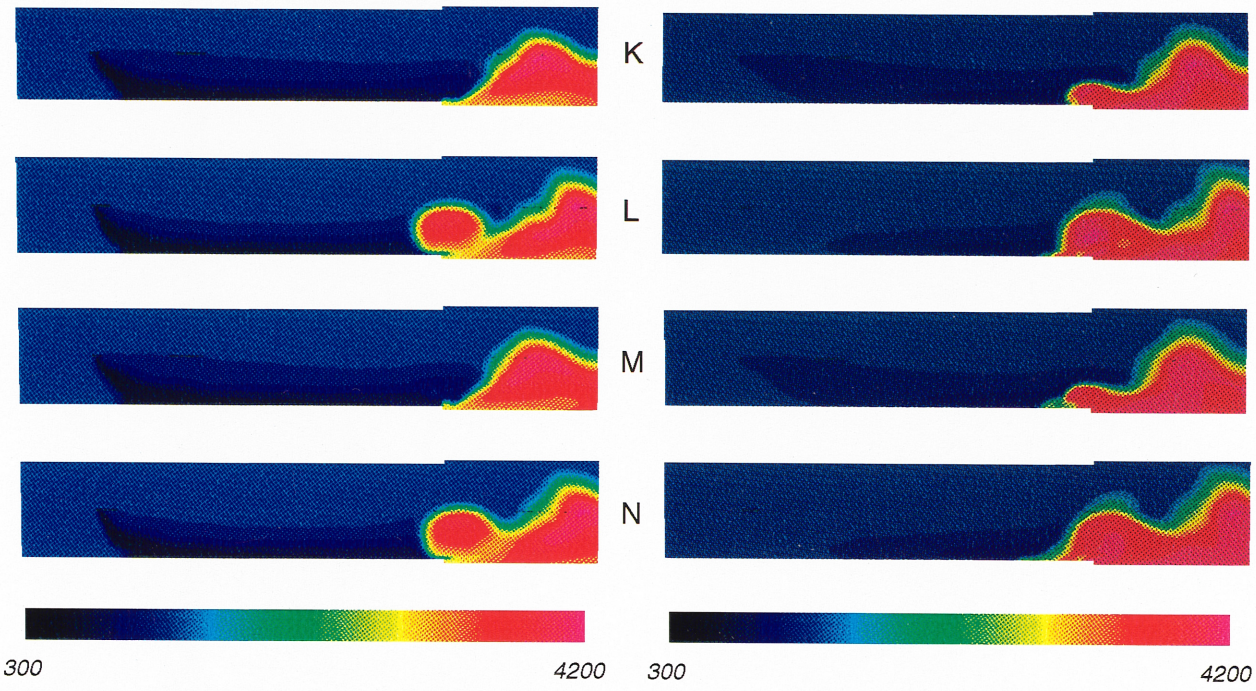

D. Temperature in Fuel Injection Plane (° F).

E. Temperature in Fuel Injection Plane + 45° (° F).

Figure 31. Flashback in 250% Baseline Diameter Mixer Tube ($\mathring{m}_{air}$ = constant) (Continued).

REPORT DOCUMENTATION PAGE

Form Approved
OMB No. 0704-0188

1. AGENCY USE ONLY (*Leave blank*)	2. REPORT DATE	3. REPORT TYPE AND DATES COVERED
	July 2004	Final Contractor Report

4. TITLE AND SUBTITLE

Analysis of Fuel Vaporization, Fuel-Air Mixing, and Combustion in Integrated Mixer-Flame Holders

5. FUNDING NUMBERS

WBS–22–714–09–46
NAS3–27235

6. AUTHOR(S)

J.M. Deur and M.C. Cline

7. PERFORMING ORGANIZATION NAME(S) AND ADDRESS(ES)

NYMA, Inc.
2001 Aerospace Parkway
Brook Park, OH 44142

8. PERFORMING ORGANIZATION REPORT NUMBER

E–14610

9. SPONSORING/MONITORING AGENCY NAME(S) AND ADDRESS(ES)

National Aeronautics and Space Administration
Washington, DC 20546–0001

10. SPONSORING/MONITORING AGENCY REPORT NUMBER

NASA CR—2004-213116

11. SUPPLEMENTARY NOTES

This research was originally published internally as HSR031 in April 1996. Responsible person, Diane Chapman, organization code 2100, 216–433–2309.

12a. DISTRIBUTION/AVAILABILITY STATEMENT

Unclassified - Unlimited
Subject Categories: 01 and 07 Distribution: Nonstandard

Available electronically at http://gltrs.grc.nasa.gov

This publication is available from the NASA Center for AeroSpace Information, 301–621–0390.

12b. DISTRIBUTION CODE

13. ABSTRACT ***(Maximum 200 words)***

Requirements to limit pollutant emissions from the gas turbine engines for the future High-Speed Civil Transport (HSCT) have led to consideration of various low-emission combustor concepts. One such concept is the Integrated Mixer-Flame Holder (IMFH). This report describes a series of IMFH analyses performed with KIVA-II, a multi-dimensional CFD code for problems involving sprays, turbulence, and combustion. To meet the needs of this study, KIVA-II's boundary condition and chemistry treatments are modified. The study itself examines the relationships between fuel vaporization, fuel-air mixing, and combustion. Parameters being considered include: mixer tube diameter, mixer tube length, mixer tube geometry (converging-diverging versus straight walls), air inlet velocity, air inlet swirl angle, secondary air injection (dilution holes), fuel injection velocity, fuel injection angle, number of fuel injection ports, fuel spray cone angle, and fuel droplet size. Cases are run with and without combustion to examine the variations in fuel-air mixing and potential for flashback due to the above parameters. The degree of fuel-air mixing is judged by comparing average, minimum, and maximum fuel/air ratios at the exit of the mixer tube, while flame stability is monitored by following the location of the flame front as the solution progresses from ignition to steady state. Results indicate that fuel-air mixing can be enhanced by a variety of means, the best being a combination of air inlet swirl and a converging-diverging mixer tube geometry. With the IMFH configuration utilized in the present study, flashback becomes more common as the mixer tube diameter is increased and is instigated by disturbances associated with the dilution hole flow.

14. SUBJECT TERMS

Propulsion; Aero gas turbine engines; Integrated mixer-flame holder; Fuel vaporization; Fuel-air mixing; Combustion

15. NUMBER OF PAGES

38

16. PRICE CODE

17. SECURITY CLASSIFICATION OF REPORT	18. SECURITY CLASSIFICATION OF THIS PAGE	19. SECURITY CLASSIFICATION OF ABSTRACT	20. LIMITATION OF ABSTRACT
Unclassified	Unclassified	Unclassified	